Deficiency in Bhlhe40 impairs resistance to *H. polygyrus bakeri* and reveals novel Csf2rb-dependent regulation of anti-helminth immunity

Nicholas N. Jarjour[1], Tara R. Bradstreet[1], Elizabeth A. Schwarzkopf[1], Melissa E. Cook[1], Chin-Wen Lai[1], Stanley Ching-Cheng Huang[1†], Reshma Taneja[2], Thaddeus S. Stappenbeck[1], Steven J. Van Dyken[1], Joseph F. Urban, Jr.[3], Brian T. Edelson[1]*

[1]Department of Pathology and Immunology, Washington University School of Medicine, St. Louis, MO 63110. USA

[2]Department of Physiology, Yong Loo Lin School of Medicine, National University of Singapore, Singapore 117597. Singapore

[3]United States Department of Agriculture (USDA), Agricultural Research Service, Beltsville Human Nutrition Research Center, Diet, Genomics, and Immunology Laboratory, Beltsville, MD 20705. USA

[†]Present address: Department of Pathology, Case Western Reserve University School of Medicine, Cleveland, OH 44106. USA

*Corresponding author. Email: bedelson@path.wustl.edu

ABSTRACT

The cytokines GM-CSF and IL-5 are thought to possess largely divergent functions despite a shared dependence on the common beta (β_C) chain to initiate signaling. Although IL-5 is part of the core type 2 cytokine signature and is required for protection against some helminths, it is dispensable for immunity to others, such as *Heligmosomoides polygyrus bakeri* (*H. polygyrus*). Whether this is due to compensatory mechanisms is unclear. The transcription factor Bhlhe40 has been shown to control GM-CSF production and is proposed to be a novel regulator of T helper type 2 cells. We have found that Bhlhe40 is required in T cells for a protective memory response to secondary *H. polygyrus* infection. *H. polygyrus* rechallenge elicited dramatic Bhlhe40-dependent changes in gene and cytokine expression by lamina propria $CD4^+$ T cells and *in vitro*-polarized T_H2 cells, including induction of GM-CSF and maximal production of type 2 cytokines including IL-5. β_C chain-deficient, but not GM-CSF-deficient, mice rechallenged with *H. polygyrus* had severely impaired protective immunity. Our results demonstrate that Bhlhe40 is an essential regulator of T_H2 cell immunity during helminth infection and reveal unexpected redundancy of β_C chain-dependent cytokines.

INTRODUCTION

Helminthic worms are parasites of eukaryotic organisms which manipulate the immune system to establish chronic infections in diverse sites, often resulting in significant tissue damage (*1-4*). A stereotypical helminth infection results in production of alarmins including IL-25, IL-33, and thymic stromal lymphopoietin (TSLP), which in turn stimulate the development of type 2 immunity characterized by production of IL-4, IL-5, and IL-13 (*1, 2, 4*). The helminth *Heligmosomoides polygyrus bakeri* (hereafter *H. polygyrus*) is a natural pathogen of mice and

has been frequently employed as a model helminth infection (*1-3, 5*). Several cytokines contribute to protective immunity against *H. polygyrus*, including IL-4 and IL-25, while IL-5, IL-33, and TSLP are considered dispensable for control of this infection (*6-9*).

However, in many instances of type 2 immunity, IL-5 plays a crucial role (*10, 11*), including in some helminth infections (*2, 4, 12*). Controversy previously existed as to whether IL-5 was protective against helminths, but it is now appreciated that deficiency in IL-5 only affects immunity to select parasites and sometimes in a life cycle stage-dependent manner (*4, 12*). IL-5 binds to the unique IL-5Rα chain paired with the common beta (β_C) chain, which is shared with the receptors for GM-CSF and IL-3 (*13, 14*). This raises the possibility that redundancy within this cytokine family could render individual members dispensable during helminth infection. While IL-3 signaling is maintained in mice in the absence of the β_C chain (*Csf2rb*) through a unique beta chain (β_{IL3}, *Csf2rb2*), GM-CSF and IL-5 signaling is abrogated in *Csf2rb*$^{-/-}$ mice (*13, 14*). Despite absolute dependence on this shared receptor chain, which is largely responsible for downstream signaling (*13*), known roles for IL-5 and GM-CSF are divergent. GM-CSF has been proposed to be a central regulator of inflammation driven by T_H1 and T_H17 cells and affects both autoimmunity and infection (*15-23*). GM-CSF also contributes to pathological T_H2 responses to allergens (*24-26*). However, little is known regarding GM-CSF during type 2 infections, though it is thought to be dispensable during infection with the helminth *Nippostrongylus brasiliensis* (*27*).

The transcription factor Bhlhe40 functions in B cells, NKT cells, T cells, and tissue-resident macrophages (*28-37*). We and others have described a crucial role for Bhlhe40 as a modulator of T_H1 and T_H17 cell cytokine production in infection and autoimmunity, particularly by controlling GM-CSF and IL-10 production (*32-36, 38*). Recent studies of *in vitro*-polarized

T_H2 cells (*39*) and house dust mite (HDM)-elicited airway T_H2 cells (*40*) have identified Bhlhe40 as a potential regulator of this cell type *in vivo*. We have also recently described a role for Bhlhe40 in large peritoneal macrophages (LPMs) during type 2 immunity (*37*). Taken together, these data suggest that Bhlhe40 may regulate type 2 infections, possibly by controlling cytokine production from T cells or via a myeloid cell-intrinsic role.

Herein, we have found that Bhlhe40 and the β_C chain are essential to protective memory to secondary *H. polygyrus* infection. *Bhlhe40*$^{-/-}$ mice exhibited severe defects during rechallenge infection with *H. polygyrus* and altered intestinal pathology, which were recapitulated in *Cd4-Cre*$^{+}$ *Bhlhe40*$^{fl/fl}$, but not *LysM-Cre*$^{+}$ *Bhlhe40*$^{fl/fl}$ mice. We defined a helminth-induced gene signature in lamina propria CD4^{+} T cells, which was disrupted in the absence of Bhlhe40. *In vitro*-polarized T_H2 cells and *H. polygyrus*-elicited CD4^{+} T cells from the small intestine lamina propria exhibited Bhlhe40-dependent production of GM-CSF, and Bhlhe40-deficient CD4^{+} T cells also exhibited reduced production of IL-5 and other cytokines. Secondary infection of *Csf2rb*$^{-/-}$, but not *Csf2*$^{-/-}$, mice resulted in severely impaired protective immunity and altered intestinal pathology. Overall, Bhlhe40 serves as a pivotal regulator of the T_H2 cell transcriptional response to helminth infection, in part by modulating GM-CSF and IL-5 production, and reveals redundant roles for these cytokines not observed during deficiency of either factor alone.

RESULTS

Bhlhe40 is required for control of *H. polygyrus* rechallenge

Primary oral challenge of C57BL/6 mice with *H. polygyrus* results in chronic infection, but rechallenge evokes a protective recall response which limits infection (*41*). To assess whether

Bhlhe40 was required for immunity to *H. polygyrus*, we challenged C57BL/6 *Bhlhe40*$^{+/+}$ and *Bhlhe40*$^{-/-}$ mice with infective *H. polygyrus* larvae (L3), cured them by treatment with pyrantel pamoate, and rechallenged them with infective L3. While *Bhlhe40*$^{+/+}$ and *Bhlhe40*$^{-/-}$ mice exhibited similar parasite fecal egg burdens during primary infection, *Bhlhe40*$^{-/-}$ mice had a much higher egg burden during secondary infection as compared to *Bhlhe40*$^{+/+}$ mice **(Fig. 1A)**. While there was a trend towards increased adult worm burden in *Bhlhe40*$^{-/-}$ as compared to *Bhlhe40*$^{+/+}$ mice after rechallenge **(Fig. 1B)**, this did not reach statistical significance, indicating that their increased egg burden was primarily due to increased worm fecundity. *H. polygyrus*-rechallenged *Bhlhe40*$^{+/+}$ and *Bhlhe40*$^{-/-}$ mice had dramatically different pathology. Type 2 granulomas can form around developing parasites and have been correlated with protective immunity (*41*). Small intestines from *Bhlhe40*$^{+/+}$ mice exhibited many granulomas, while those from *Bhlhe40*$^{-/-}$ mice resembled healthy tissue **(Fig. 1, C and D)**. Histological analysis and immunostaining showed reduced immune infiltration and damage to the smooth muscle layer in *H. polygyrus*-rechallenged *Bhlhe40*$^{-/-}$ as compared to *Bhlhe40*$^{+/+}$ mice **(Fig. 1, E and F)**.

When we explored the cellular composition of the small intestine lamina propria (SILP) following *H. polygyrus* rechallenge of *Bhlhe40*$^{+/+}$ mice by flow cytometry, we found both CD45^{+}CD64^{+}F4/80^{+}MHC-II^{+}Ly6C^{-} resident macrophages (*42*, *43*) and another CD45^{+}F4/80^{+}CD64^{+}MHC-II^{lo}Ly6C^{lo} autofluorescent population, which we termed granuloma-associated monocytes/macrophages (GMMs) **(Fig. 2, A and B)**. This latter population may correspond to previously described clodronate-sensitive alternatively activated macrophages seen by immunostaining during *H. polygyrus* infection (*44*). SILP CD45^{+}F4/80^{+}CD64^{-}CD11b^{+}SSC-A^{hi} eosinophils were also significantly increased after secondary *H. polygyrus* infection **(Fig. 2, A and B and fig. S1A)**. However, GMMs and eosinophils were greatly reduced in *H. polygyrus*-

rechallenged *Bhlhe40*$^{-/-}$ as compared to *Bhlhe40*$^{+/+}$ mice, in contrast to SILP CD3^{+} T cells **(Fig. 2, A and B and fig. S1B)**. Because *H. polygyrus* infection is known to change the cellular composition of the peritoneal cavity (*4, 45, 46*), we assessed accumulation of LPMs and peritoneal eosinophils, and found severe reductions in both populations in *H. polygyrus*-rechallenged *Bhlhe40*$^{-/-}$ as compared to *Bhlhe40*$^{+/+}$ mice, as well as impaired LPM polarization as assessed by RELMα staining **(Fig. 2, C to E and fig. S1, C to E)**. In contrast, serum *H. polygyrus*-specific IgG1 titers were not affected by loss of Bhlhe40 **(fig. S1F)**. These data indicated impaired responses by multiple myeloid cell lineages to *H. polygyrus* rechallenge in *Bhlhe40*$^{-/-}$ mice.

Bhlhe40 is required in T cells for a normal immune response to *H. polygyrus*

We next employed *Cd4-Cre*$^{+}$ *Bhlhe40*$^{fl/fl}$ and *LysM-Cre*$^{+}$ *Bhlhe40*$^{fl/fl}$ mice to address whether loss of Bhlhe40 specifically in T cells or myeloid cells recapitulated the phenotype of *Bhlhe40*$^{-/-}$ mice during secondary *H. polygyrus* infection. *Cd4-Cre*$^{+}$ *Bhlhe40*$^{fl/fl}$ mice were severely impaired in controlling *H. polygyrus* rechallenge and lacked intestinal granulomas as compared to *Cd4-Cre*$^{-}$ *Bhlhe40*$^{fl/fl}$ mice **(Fig. 3, A and B)**. When we assessed the response of myeloid cells to secondary infection, we found that loss of Bhlhe40 selectively in T cells was sufficient to perturb both the SILP and peritoneal responses **(Fig. 3, C to F)**. In contrast, *LysM-Cre*$^{+}$ *Bhlhe40*$^{fl/fl}$ mice were able to control infection and formed intestinal granulomas comparably to *LysM-Cre*$^{-}$ *Bhlhe40*$^{fl/fl}$ mice **(Fig. 3, G and H)**. Therefore, Bhlhe40 expression was required in T cells to control secondary *H. polygyrus* infection, but was dispensable in LysM-expressing myeloid cells.

Bhlhe40 is required for a normal CD4$^+$ T cell transcriptional response to *H. polygyrus*

We next asked whether loss of Bhlhe40 dysregulated CD4$^+$ T cell gene expression in response to *H. polygyrus* rechallenge. To address this, we sorted CD4$^+$ T cells from the SILP of naïve and rechallenged *Bhlhe40*$^{+/+}$ and *Bhlhe40*$^{-/-}$ mice for gene expression microarrays. By comparing CD4$^+$ T cells from naïve and *H. polygyrus*-rechallenged *Bhlhe40*$^{+/+}$ mice, we defined a helminth-induced signature which included transcripts for cytokines (including *Areg*, *Il3*, *Il4*, *Il5*, *Il6*, *Il13*, *Csf1*, *Csf2*, *Lif*, *Tnf*, *Tnfsf11*), cytokine receptors (including *Il1rl1*, *Il1r2*, *Il17rb*), and transcription factors (including *Atf3*, *Bhlhe40*, *Gata3*, *Nfil3*, *Pparg*, *Rbpj*, *Vdr*, and *Zeb2*) **(Fig. 4A and fig. S2A)**. When we assessed Bhlhe40-dependent genes after *H. polygyrus* rechallenge, we found that a significant majority were part of the helminth-induced signature and that Bhlhe40-dependent genes were distinct in CD4$^+$ T cells from naïve and *H. polygyrus*-rechallenged mice **(Fig. 4, B and C and fig. S2, B and C)**. When we used gene set enrichment analysis (GSEA) to look for Bhlhe40-dependent gene modules, we noted that two of the most enriched sets in *Bhlhe40*$^{+/+}$ as compared to *Bhlhe40*$^{-/-}$ CD4$^+$ T cells after *H. polygyrus* rechallenge were “growth factor activity” and “cytokine activity,” reflecting altered expression of cytokine genes including *Areg*, *Il5*, *Il6*, *Il13*, *Csf1*, *Csf2*, and *Lif*, but not *Il3*, *Il4*, or *Tnf* **(Fig. 4, D and E)**. Furthermore, when we assessed differential expression of the lineage-specifying transcription factors of each T helper cell subset as well as a recently defined set of transcriptional regulators of *in vitro*-polarized T_H2 cells (*39*), we observed reduced expression of *Pparg* in *Bhlhe40*$^{-/-}$ as compared to *Bhlhe40*$^{+/+}$ CD4$^+$ T cells from *H. polygyrus*-rechallenged mice (2.4-fold reduced), but only subtle changes in other factors including *Gata3* (1.4-fold reduced) **(Fig. 4E)**. *Bhlhe40* expression was markedly induced in mice experiencing secondary infection as compared to naïve mice **(Fig. 4E)**. Using *Bhlhe40*^{GFP} bacterial artificial chromosome

reporter mice (*34*), we observed a marked increase in SILP GFP$^+$ CD4$^+$ T cells after *H. polygyrus* rechallenge **(Fig. 4F)**. Taken together, these data showed that Bhlhe40 was induced by SILP CD4$^+$ T cells in response to *H. polygyrus* rechallenge and was critical for their normal transcriptional program.

Loss of Bhlhe40 impairs T cell cytokine production in response to *H. polygyrus*

Next, we restimulated SILP cells from naïve and rechallenged *Cd4-Cre$^-$ Bhlhe40$^{fl/fl}$* and *Cd4-Cre$^+$ Bhlhe40$^{fl/fl}$* mice *ex vivo* with phorbol 12-myristate 13-acetate (PMA) and ionomycin to assess cytokine production. Rechallenge with *H. polygyrus* induced production of IL-4, IL-5, and IL-13 from *Cd4-Cre$^-$ Bhlhe40$^{fl/fl}$* and *Cd4-Cre$^+$ Bhlhe40$^{fl/fl}$* CD4$^+$ T cells; however, Bhlhe40 was required for normal frequencies of single- and multi-cytokine-producing cells, largely due to reductions in IL-5$^+$ and IL-13$^+$ CD4$^+$ T cells **(Fig. 5, A to C)**. Because *Csf2* was upregulated by *H. polygyrus* rechallenge in a Bhlhe40-dependent fashion, we also assessed GM-CSF and found that it was markedly induced by rechallenge (~35% of *Cd4-Cre$^-$ Bhlhe40$^{fl/fl}$* CD4$^+$ T cells) and that this required Bhlhe40 (~10% of *Cd4-Cre$^+$ Bhlhe40$^{fl/fl}$* CD4$^+$ T cells) **(Fig. 5, D and E)**. T_H2 cells disseminate widely in mice infected with *H. polygyrus* (*45, 46*). CD4$^+$ T cell cytokine responses in the peritoneal cavity and mesenteric lymph nodes from *H. polygyrus*-rechallenged *Cd4-Cre$^-$ Bhlhe40$^{fl/fl}$* and *Cd4-Cre$^+$ Bhlhe40$^{fl/fl}$* mice were generally consistent with those in the SILP **(fig. S3)**. To assess whether Bhlhe40 was also required for normal cytokine production by a pure population of T_H2 cells, we differentiated naïve splenic CD4$^+$ T cells into T_H2 cells and restimulated them to assess cytokine production. We found that Bhlhe40 was essential for production of GM-CSF and that loss of Bhlhe40 also impaired *in vitro* production of type 2

cytokines **(fig. S4)**. Therefore, these data indicated that Bhlhe40 is required *in vitro* and *in vivo* for normal T_H2 cell function.

As Bhlhe40 is a known repressor of IL-10 (*32-34, 36*), we also assessed IL-10 production from SILP $CD4^+$ T cells. Indeed, SILP $CD4^+$ T cells lacking Bhlhe40 produced significantly higher levels of IL-10 after *H. polygyrus* rechallenge **(fig. S5A)**. Nevertheless, genetic deletion of IL-10 in *Bhlhe40*$^{-/-}$ *Il10*$^{-/-}$ mice was not sufficient to restore control of infection or normal intestinal granulomatous pathology **(fig. S5, B and C)**. Collectively, these data demonstrated a key role for Bhlhe40 in $CD4^+$ T cell cytokine responses to helminth infection, notably controlling production of the β_C chain family cytokines IL-5 and GM-CSF.

Loss of the β_C chain impairs protective memory to *H. polygyrus*

As protective memory responses to *H. polygyrus* rechallenge are unaffected by IL-5 blockade (*6*), we first asked whether loss of GM-CSF signaling was sufficient to impair control of a secondary infection with *H. polygyrus*. Genetic deletion of GM-CSF (*Csf2*$^{-/-}$ mice) did not result in severe defects in control of *H. polygyrus* infection as compared to *Csf2*$^{+/+}$ mice **(fig. S6, A to F)**. As IL-5 and GM-CSF were individually dispensable, we then rechallenged *Csf2rb*$^{+/+}$ and *Csf2rb*$^{-/-}$ mice. Remarkably, *Csf2rb*$^{-/-}$ mice had a severe defect in control of *H. polygyrus* as compared to *Csf2rb*$^{+/+}$ mice **(Fig. 6A)**. *Csf2rb*$^{-/-}$ mice did not form intestinal granulomas or develop a normal SILP myeloid cell response to *H. polygyrus* rechallenge as compared to *Csf2rb*$^{+/+}$ mice **(Fig. 6, B and C)**. Furthermore, loss of the β_C chain resulted in defects in peritoneal myeloid cell responses similar to those seen in *Bhlhe40*$^{-/-}$ and *Cd4-Cre*$^+$ *Bhlhe40*$^{fl/fl}$ mice **(Fig. 6, D to F)**. To exclude a role for β_C chain-dependent IL-3 signaling, we singly

blocked GM-CSF or IL-5 signaling with neutralizing antibodies or blocked both cytokines together. Double, but not single, blockade resulted in severely impaired protective immunity **(fig. S6, G and H).** Taken together, these data indicated that IL-5 and GM-CSF were collectively, but not individually, critical to control of *H. polygyrus* rechallenge.

DISCUSSION

We have demonstrated that protective memory responses against *H. polygyrus* are critically dependent on Bhlhe40 and the β_C chain. Bhlhe40 is specifically required in $CD4^+$ T cells to promote a normal myeloid cell response to *H. polygyrus* by supporting expression of cytokine transcripts as well as other potential regulators of helminth infection, including *Areg*, *Csf2*, *Il5*, *Il13*, *Nlrp3*, and *Pparg* (*47-49*). We have also described the $CD4^+$ T cell transcriptome within the SILP during secondary *H. polygyrus* infection. These data provide unique insight into the $CD4^+$ T cell global transcriptional response to helminths at the site of infection. We found that Bhlhe40 is a key regulator of T_H2 cell cytokine production. Notably, GM-CSF and IL-5 were markedly stimulated by *H. polygyrus* rechallenge and this response was Bhlhe40-dependent. In light of these data, we assessed the importance of the β_C chain during *H. polygyrus* rechallenge and found that it was critically required for protective immunity, despite control of secondary *H. polygyrus* infection during IL-5 blockade (this manuscript and (*6*)), during GM-CSF blockade, and in *Csf2*$^{-/-}$ mice. These data support redundant roles for Bhlhe40-dependent β_C chain-dependent cytokines in protective immunity to *H. polygyrus*.

When we compared differentially expressed transcripts between *H. polygyrus*-elicited and naive SILP $CD4^+$ T cells, we found a remarkable similarity to the transcriptional profile of

HDM-elicited airway T_H2 cells (*Bhlhe40*, *Cd200r1*, *Il6*, *Plac8*, *Igfbp7*) (*40*), demonstrating significant conservation of the T_H2 transcriptional program independent of tissue environment and stimulus. When we assessed whether Bhlhe40 was functionally required in T cells during type 2 immunity, we found that SILP $CD4^+$ T cells activated by *H. polygyrus* rechallenge required Bhlhe40 for normal expression of many helminth-induced genes and to control helminth rechallenge. We therefore demonstrate for the first time that Bhlhe40 regulates *in vivo* T_H2 cell responses, consistent with a recent screen for novel regulators of *in vitro*-polarized T_H2 cells that identified Bhlhe40 (*39*). Notably, *Pparg* expression was reduced in the absence of Bhlhe40, and as PPARγ is required for normal T_H2 cell responses and protective immunity to *H. polygyrus*, this may indicate that some of the effects of Bhlhe40 deficiency are indirect (*47,50*). Our work and that of others has now established key roles for Bhlhe40 in T_H1, T_H2, and T_H17 cells as a pivotal regulator of GM-CSF, IL-10, and other cytokines (*32-36, 38*). These data and a recent study on c-Maf (*51*) suggest that T cell production of many cytokines may be controlled by multi-lineage transcription factors in addition to lineage-restricted factors. In light of the critical role for Bhlhe40 in multiple $CD4^+$ T cell subsets, clinical targeting of factors regulating Bhlhe40 may possess significant therapeutic potential.

While GM-CSF and IL-5 have long been known to share common signaling through the β_C chain, their described functions are largely distinct, with GM-CSF contributing to T_H1 and T_H17 cell-driven inflammation and IL-5 contributing to type 2 immunity (*10, 11, 16, 52*). We have demonstrated that protective memory to a helminth infection unaffected by IL-5 blockade and also insensitive to GM-CSF deficiency is nonetheless dependent on the combination of GM-CSF and IL-5 signaling through the β_C chain. It remains to be determined how GM-CSF and IL-5 compensate for each other, whether by direct substitution or via effects on distinct arms of the

type 2 response. While redundancy between β_C chain family cytokines is not well described, it is known that these cytokines can regulate eosinophils in a complementary manner (*53*). Future studies should establish whether GM-CSF and IL-5 are collectively involved in protective immunity to other helminth infections. As β_{IL3} chain-dependent IL-3 signaling is preserved in *Csf2rb*$^{-/-}$ mice (*13, 14*), it is also of interest to establish whether additionally blocking IL-3 results in a more severe defect in immunity to *H. polygyrus* than is observed in *Csf2rb*$^{-/-}$ mice. IL-3 regulates basophilia in response to *H. polygyrus* and basophils help control infection with this helminth (*54, 55*), suggesting that IL-3 is likely important for control of *H. polygyrus* infection.

Our findings reveal novel transcriptional and cytokine regulation of the immune response to helminth infection, elucidating a critical function for Bhlhe40 during *in vivo* T_H2 cell immunity and an unexpected role for β_C chain-dependent signaling. Our data suggest that the importance of β_C chain family cytokines may have been underestimated in type 2 diseases because of redundancy. Further studies are needed to elucidate whether compensation between β_C chain family cytokines is a general theme of type 2 immunity and whether combinatorial targeting of these factors could yield improved clinical outcomes in diseases of pathological type 2 immunity.

MATERIALS AND METHODS

Mice

C57BL/6 (Taconic and Jackson), *Il10*$^{-/-}$ (B6.129P2-Il10tm1Cgn/J, Jackson), *Csf2*$^{-/-}$ (B6.129S-*Csf2*^{tm1Mlg}/J, Jackson), *Csf2rb*$^{-/-}$ (B6.129S1-*Csf2rb*^{tm1Cgb}/J, Jackson), *Cd4-Cre* (B6.Cg-Tg(Cd4-cre)1Cwi/BfluJ, Jackson) and *LysM-Cre* (B6N.129P2(B6)-*Lyz2*$^{tm1(cre)Ifo}$/J, Jackson) mice were obtained from the vendors listed. *Bhlhe40*$^{-/-}$ (10 generations backcrossed to the C57BL/6

background) (*33, 56*), *Bhlhe40*$^{GFP+}$ (10 generations backcrossed to the C57BL/6 background) (*34*), and *Bhlhe40*$^{fl/fl}$ (*32*) mice have been previously reported. All mice were maintained in our specific pathogen free animal facility. Sex-matched littermates were used for experiments whenever possible. Experiments with *Csf2*$^{-/-}$ and *Csf2rb*$^{-/-}$ mice used cohoused, age-matched, sex-matched C57BL/6 controls bred in our animal facility or purchased from Jackson. All animal experiments were approved by the Animal Studies Committee of Washington University in St. Louis.

***Heligmosomoides polygyrus bakeri* infections**

Infective *Heligmosomoides polygyrus bakeri* third-stage larvae (L3) were prepared as described (*5*). For both primary and secondary infection, mice were orally gavaged with 200 L3 with a 20-gauge ball-tipped gavage needle. Female mice were used for experiments whenever possible. Fecal samples were collected at 8, 11, 14, and 21 days after primary and secondary infection and weighed. Eggs were counted by dissolution of feces in 5 ml water, followed by a 1:1 dilution with a saturated sodium chloride solution before loading into a McMaster counting chamber (Chalex LLC). For rechallenge experiments, mice were cleared of infection by oral gavage with 2 mg of pyrantel pamoate (Columbia Laboratories) diluted in Dulbecco's PBS on days 14 and 15 after primary infection and were rested for 3-4 weeks before reinfection. Blood was collected at day 21 post-rechallenge and allowed to clot for >1 hour before serum collection by centrifugation at 1,500 g for 15 minutes. Mice were sacrificed on day 17 or 22 of secondary infection for assessment of cellular responses. Macroscopic granulomas present at day 22 of secondary infection that were visible to the naked eye were counted along the length of the intact intestines. Assessment of the intestinal worm burden was performed at day 17 or 22 of primary

or secondary infection. Adult worms were collected by cutting the intestine open and into ~4 in sections, placing the tissue and contents into a metal filter on top of a 50 ml tube of PBS, and setting the tube in a 37 ºC water bath. Worms then actively migrated through the filter over several hours and sedimented. Worms were counted visually in petri dishes.

In vivo antibody blockade

Mice were infected, cleared, and rested as above. Immediately before reinfection, mice were injected i.p. with 300 µg of αGM-CSF (Leinco, G670, clone MP1-22E9), 300 ug of αIL-5 (BioXCell, BE0198, clone TRFK5), or control polyclonal rat IgG (Sigma Aldrich, I4131) and were given the same dose i.p. every other day until sacrifice (*52*).

In vitro T_H2 cell culture

The EasySep mouse naïve CD4+ T cell isolation kit (Stemcell Technologies, 19765A) was used to isolate T cells from the spleens of untreated mice. Cells were cultured in complete Iscove's modified Dulbecco's media (cIMDM, with added 10 % FBS, L-glutamine, sodium pyruvate, non-essential amino acids, penicillin/streptomycin, and β-mercaptoethanol) in flat-bottom, tissue culture-treated 48 well plates with plate-bound anti-CD3 and anti-CD28. Plates were coated overnight with anti-CD3 antibody (BioXCell, 2 µg/mL, clone 145-2C11) and anti-CD28 antibody (BioLegend, 2 µg/ml, clone 37.51) before use. To polarize naïve T cells to T_H2 cells, IL-4 (BioLegend, 10 ng/mL) and anti-IFN-γ (Leinco, 5 µg/mL, clone H22) were added at the start of culture. Cells were split at day 3, and on day 4 cells were stimulated for 24 hours with plate-bound anti-CD3 and anti-CD28 (coated as above) for assessment of secreted cytokines in the supernatant by ELISA.

Enzyme-linked immunosorbent assay (ELISA)

Nunc Maxisorp plates were coated with capture antibodies (for cytokine ELISAs) or *H. polygyrus* lysate (for *H. polygyrus*-specific IgG1 ELISA) overnight. Wells were washed with PBS-Tween 20 (0.05%), and 1% BSA in PBS was added for one hour to block. After washing, culture supernatants (cytokine ELISAs) or serum (IgG1 ELISA) were added for 1-2 hours, except for the GM-CSF ELISA (overnight). After washing, cytokine-detection biotinylated antibodies or horseradish peroxidase (HRP)-conjugated anti-mouse IgG1 antibody were added for 1 hour, except for the GM-CSF ELISA (2 hours). For cytokine ELISAs, following another wash, streptavidin-conjugated horseradish peroxidase (HRP) was added for 1 hour. After washing, a 1:1 mixture of room temperature TMB A and B solutions (BD OptEIA) was added. The reaction was stopped with 1 M H_3PO_4. Samples were analyzed on an iMark microplate reader (BioRad). For cytokine ELISAs, standard curves were generated with purified cytokines. For the IgG1 ELISA, serum was diluted between 10^{-2} and 10^{-8} and the last well with an OD_{450} above 0.100 represented the titer. ELISA reagents are listed in Table S1.

To generate *H. polygyrus* lysate, adult worms collected as above were washed repeatedly in PBS, and ground in a Dounce homogenizer in 1 mL of PBS. Debris was then pelleted by centrifugation at 16,000 g for 20 minutes at 4 ºC. The supernatant was passed through a 0.2 µm filter and stored at -80 ºC. Lysate was titrated for an ELISA with the serum of *H. polygyrus*-rechallenged mice, and the greatest dilution of lysate (1:1000) which yielded maximal signal was used.

Brightfield and epifluorescence microscopy

The proximal 6 cm of the small intestine were formed into a swiss roll (*57*) and were frozen in OCT media. 10 μm cryosections were cut using a Leica CM1950 cryostat. For hematoxylin and eosin staining, sections were fixed in 4% PFA, washed, and stained. For immunofluorescent staining, sections were fixed in acetone, washed, and blocked with CAS-Block (Invitrogen). Staining was performed with Cy3-anti-α-smooth muscle actin (clone 1A4, Sigma) and AlexaFluor647-anti-F4/80 (clone BM8, BioLegend) diluted in CAS block, followed by washing. Sections were mounted with Abcam Fluoroshield Mounting Medium with DAPI. All images were captured with a Nikon Eclipse E800 microscope equipped with a MicroPublisher 5.0 RTV camera (QImaging) for brightfield microscopy and an EXi Blue camera (QImaging) for fluorescence microscopy using QCapture software (QImaging). Fluorescence images were merged and levelled in Adobe Photoshop.

Leukocyte collection from tissues

Peritoneal cells were collected from body cavities by lavage. Mesenteric lymph nodes and spleens were harvested into cIMDM, homogenized through a 70 μm filter, and washed. Isolation of small intestine lamina propria cells was performed as described (*58*). In brief, 4 cm of the proximal small intestine were excised, cleaned of fecal contents, and cut into 2-3 pieces. The tissue was shaken twice in 1x HBSS (with added HEPES, 10% FBS, EDTA, and DTT) for 20 minutes to remove the epithelial layer. The tissue was then shaken at 220 rpm at 37 ºC for 1 hour in an Innova 4330 shaker (New Brunswick Scientific) with Collagenase IV (Sigma, C5138) in RPMI 1640 (with added 10% FBS, L-glutamine, penicillin/streptomycin, and 2-mercaptoethanol). Cells were then pelleted by centrifugation and washed.

All cells were passed through a 70 μm cell strainer before analysis. If necessary, tissues were treated with ACK lysis buffer to lyse red blood cells. Cells were counted with a hemocytometer using trypan blue.

Flow cytometry

Cell surface staining was conducted in PBS with 0.5% BSA and 2 mM EDTA (hereafter FACS buffer) with or without 0.02% sodium azide. In brief, cells were washed in FACS buffer, blocked with α-CD16/32 (clone 2.4G2, BioXCell) for 5-10 minutes at 4 ºC, stained for 20 minutes at 4 ºC, and washed with FACS buffer before flow cytometry. Flow cytometry was performed on LSRFortessa X20, FACSCanto II, and LSR II instruments (all BD). Analysis was performed with FlowJo software (Treestar). Antibodies and fluorescent dyes used in this study are listed in Table S1.

Gating of cell populations was as follows (all analysis pre-gated on FSC/SSC followed by a FSC-W/FSC-A singlet gate). SILP macrophages were gated as $CD45^{+}F4/80^{+}CD64^{+}MHC\text{-}II^{+}Ly6C^{-}$, while GMMs were gated as $CD45^{+}F4/80^{+}CD64^{+}MHC\text{-}II^{lo}Ly6C^{lo}$. SILP eosinophils were gated as $CD45^{+}F4/80^{+}CD64^{-}CD11b^{+}SSC\text{-}A^{hi}$, and this approach was validated in some experiments with Siglec-F staining. SILP $CD3^{+}$ T cells were gated as $CD45^{+}F4/80^{-}CD64^{-}CD19^{-}CD3^{+}$. SILP $CD4^{+}$ T cells were gated as $CD19^{-}F4/80^{-}TCR\beta^{+}CD4^{+}CD8^{-}$. LPMs were gated as $CD115^{+}CD11b^{+}ICAM2^{+}MHC\text{-}II^{lo}$. Peritoneal eosinophils were gated as $Siglec\text{-}F^{+}ICAM2^{-}$. Peritoneal $CD4^{+}$ T cells were gated as $ICAM2^{-}TCR\beta^{+}CD4^{+}CD8^{-}$. Mesenteric lymph node $CD4^{+}$ T cells were gated as $CD19^{-}TCR\beta^{+}CD4^{+}CD8^{-}$.

Intracellular staining for flow cytometry

For intracellular cytokine staining of T cells, total SILP, peritoneal, and mesenteric lymph node cells were cultured at 0.5-1 million cells/well in a 96 well V-bottom non-tissue culture-treated plate for 3-4 hours at 37 °C with 8% CO_2 in the presence of PMA (50 ng/ml), ionomycin (1 μM), and brefeldin A (1 μg/ml) in cIMDM. Cells were then surface stained and fixed with 4% paraformaldehyde (PFA). Cells were then washed with FACS buffer and stored overnight. To permeabilize the cells, samples were washed with 1x Perm/Wash buffer (BD, 554714) and stained for 20 minutes at 4 ºC, followed by washing in 1x Perm/Wash buffer and FACS buffer before flow cytometry.

For RELMα staining, the BioLegend True-Nuclear Transcription Factor Buffer set (424401) was used. After surface staining, cells were fixed with 1x Fix Concentrate buffer in Fix Diluent for 30 minutes at 4 ºC. Cells were then washed with FACS buffer and stored overnight. Samples were washed with 1x Perm buffer diluted in water for permeabilization. After blocking with 2% rat serum, samples were stained for 1 hour at RT with anti-RELMα antibody followed by washing in 1x Perm buffer, staining with secondary antibody for 20 min at 4 ºC, washing in 1x Perm buffer, and washing in FACS buffer before flow cytometry.

Microarrays

Singlet F4/80$^-$ TCRβ$^+$ CD4$^+$ CD8$^-$ SILP cells were sorted from naïve and *H. polygyrus*-rechallenged mice using a FACSAria II (BD) into FBS, followed by lysis and RNA purification using the E.Z.N.A. MicroElute Total RNA kit (Omega Bio-Tek). RNA was submitted to the Genome Technology Access core at Washington University for cDNA synthesis (NuGen Pico SL) followed by analysis on the Affymetrix Mouse Gene 1.0 ST microarray platform. Data were analyzed with the DNASTAR ArrayStar program. All CEL files were normalized together.

Genes with an expression value of >5 (in log 2 scale) in at least one replicate were considered expressed. For generation of lists of differentially expressed genes at a ≥2-fold differential expression cutoff between groups, p-value significance of ≤0.01 by the moderated *t*-test was also required. Morpheus was used to generate heatmaps (software.broadinstitute.org/morpheus/). The Venn Diagram Plotter tool (Pacific Northwest National Laboratories, omics.pnl.gov) was used to generate Venn diagrams. Multiple differentially expressed probe sets representing a single gene were presented in heat maps, but only unique genes were counted in Venn diagrams. To assess gene set enrichment, the GSEA software from the Broad Institute was used to analyze all expressed genes for enrichment of C5 database gene sets (*59*).

Quantification and statistical analysis

All data are from at least two independent experiments, unless otherwise indicated. Data were analyzed by unpaired two-tailed Student's *t*-tests (Prism 7; GraphPad Software, Inc.) with $p \leq 0.05$ considered significant. For relevant comparisons where no p-value is shown, the p-value was > 0.05. The NES score calculated by the GSEA software was used to account for set size effects when determining enrichment of gene sets. The GSEA-calculated FWER p value was used as a conservative measure of significance. Horizontal bars represent the mean and error bars represent the standard error of the mean (s.e.m.).

SUPPLEMENTARY MATERIALS

Fig. S1. Loss of Bhlhe40 dysregulates myeloid cell responses to *H. polygyrus* rechallenge.

Fig. S2. Bhlhe40 regulates distinct gene sets in $CD4^+$ T cells from naïve and *H. polygyrus*-rechallenged mice.

Fig. S3. Bhlhe40 is required in T cells for normal cytokine production during *H. polygyrus* rechallenge.

Fig. S4. *In vitro*-polarized T_H2 cells require Bhlhe40 for normal cytokine production.

Fig. S5. Genetic deletion of IL-10 in *Bhlhe40*$^{-/-}$ *Il10*$^{-/-}$ mice does not restore control of *H. polygyrus* rechallenge.

Fig. S6. Combined deficiency in IL-5 and GM-CSF results in impaired control of *H. polygyrus* rechallenge.

Table S1. Antibodies and fluorescent dyes.

REFERENCES AND NOTES

1. R. M. Maizels, H. H. Smits, H. J. McSorley, Modulation of Host Immunity by Helminths: The Expanding Repertoire of Parasite Effector Molecules. *Immunity* **49**, 801-818 (2018).
2. D. Sorobetea, M. Svensson-Frej, R. Grencis, Immunity to gastrointestinal nematode infections. *Mucosal Immunol* **11**, 304-315 (2018).
3. N. Patel, T. Kreider, J. F. Urban, Jr., W. C. Gause, Characterisation of effector mechanisms at the host:parasite interface during the immune response to tissue-dwelling intestinal nematode parasites. *Int. J. Parasitol.* **39**, 13-21 (2009).
4. J. E. Allen, T. E. Sutherland, Host protective roles of type 2 immunity: parasite killing and tissue repair, flip sides of the same coin. *Semin. Immunol.* **26**, 329-340 (2014).

5. M. Camberis, G. Le Gros, J. Urban, Jr., Animal model of Nippostrongylus brasiliensis and Heligmosomoides polygyrus. *Curr. Protoc. Immunol.* **Chapter 19**, Unit 19.12 (2003).
6. J. F. Urban, Jr., I. M. Katona, W. E. Paul, F. D. Finkelman, Interleukin 4 is important in protective immunity to a gastrointestinal nematode infection in mice. *Proc. Natl. Acad. Sci. U. S. A.* **88**, 5513-5517 (1991).
7. Pei, C., Zhao, C., Wang, A.J., Fan, A.X., Grinchuk, V., Smith, A., Sun, R., Xie, Y., Lu, N., Urban, J.F., Jr., et al, Critical Role for Interleukin-25 in Host Protective Th2 Memory Response against Heligmosomoides polygyrus bakeri. *Infect. Immun.* **84**, 3328-3337 (2016).
8. Massacand, J.C., Stettler, R.C., Meier, R., Humphreys, N.E., Grencis, R.K., Marsland, B.J., Harris, N.L, Helminth products bypass the need for TSLP in Th2 immune responses by directly modulating dendritic cell function. *Proc. Natl. Acad. Sci. U. S. A.* **106**, 13968-13973 (2009).
9. Zaiss, M.M., Maslowski, K.M., Mosconi, I., Guenat, N., Marsland, B.J., Harris, N.L., IL-1beta suppresses innate IL-25 and IL-33 production and maintains helminth chronicity. *PLoS Pathog.* **9**, e1003531 (2013).
10. Bagnasco, D., Ferrando, M., Varricchi, G., Puggioni, F., Passalacqua, G., Canonica, G.W., Anti-Interleukin 5 (IL-5) and IL-5Ra Biological Drugs: Efficacy, Safety, and Future Perspectives in Severe Eosinophilic Asthma. *Front. Med. (Lausanne)* **4**, 135 (2017).
11. F. Roufosse, Targeting the Interleukin-5 Pathway for Treatment of Eosinophilic Conditions Other than Asthma. *Front. Med.* **5**, 49 (2018).

12. R. M. Maizels, A., A. Balic, A., Resistance to Helminth Infection: The Case for Interleukin-5-Dependent Mechanisms. *J. Infect. Dis.* **190**, 427-429 (2004).

13. M. Dougan, G. Dranoff, S. K. Dougan, GM-CSF, IL-3, and IL-5 Family of Cytokines: Regulators of Inflammation. *Immunity* **50**, 796-811 (2019).

14. Robb, L., Drinkwater, C.C., Metcalf, D., Li, R., Kontgen, F., Nicola, N.A., Begley, C.G., Hematopoietic and lung abnormalities in mice with a null mutation of the common beta subunit of the receptors for granulocyte-macrophage colony-stimulating factor and interleukins 3 and 5. *Proc. Natl. Acad. Sci. U. S. A.* **92**, 9565-9569 (1995).

15. A. M. LeVine, J. A. Reed, K. E. Kurak, E. Cianciolo, J. A. Whitsett, GM-CSF–deficient mice are susceptible to pulmonary group B streptococcal infection. *J. Clin. Invest*. **103**, 563-569 (1999).

16. B. Becher, S. Tugues, M. Greter, GM-CSF: From Growth Factor to Central Mediator of Tissue Inflammation. *Immunity* **45**, 963-973 (2016).

17. G. S. Deepe, Jr., R. Gibbons, E. Woodward, Neutralization of endogenous granulocyte-macrophage colony-stimulating factor subverts the protective immune response to Histoplasma capsulatum. *J. Immunol.* **163**, 4985-4993 (1999).

18. Gonzalez-Juarrero, M., Hattle, J.M., Izzo, A., Junqueira-Kipnis, A.P., Shim, T.S., Trapnell, B.C., Cooper, A.M., Orme, I.M., Disruption of granulocyte macrophage-colony stimulating factor production in the lungs severely affects the ability of mice to control Mycobacterium tuberculosis infection. *J. Leukoc. Biol.* **77**, 914-922 (2005).

19. Y. Hirata, L. Egea, S. M. Dann, L. Eckmann, M. F. Kagnoff, GM-CSF-facilitated dendritic cell recruitment and survival govern the intestinal mucosal response to a mouse enteric bacterial pathogen. *Cell Host Microbe* **7**, 151-163 (2010).

20. Mandujano, J.F., D'Souza, N.B., Nelson, S., Summer, W.R., Beckerman, R.C., Shellito, J.E., Granulocyte-macrophage colony stimulating factor and Pneumocystis carinii pneumonia in mice. *Am. J. Respir. Crit. Care Med.* **151**, 1233-1238 (1995).

21. Paine, R., 3rd, Preston, A.M., Wilcoxen, S., Jin, H., Siu, B.B., Morris, S.B., Reed, J.A., Ross, G., Whitsett, J.A., Beck, J.M., Granulocyte-macrophage colony-stimulating factor in the innate immune response to Pneumocystis carinii pneumonia in mice. *J. Immunol.* **164**, 2602-2609 (2000).

22. Y. Zhan, G. J. Lieschke, D. Grail, A. R. Dunn, C. Cheers, Essential roles for granulocyte-macrophage colony-stimulating factor (GM-CSF) and G-CSF in the sustained hematopoietic response of Listeria monocytogenes-infected mice. *Blood* **91**, 863-869 (1998).

23. Croxford, A.L., Lanzinger, M., Hartmann, F.J., Schreiner, B., Mair, F., Pelczar, P., Clausen, B.E., Jung, S., Greter, M., Becher, B., The Cytokine GM-CSF Drives the Inflammatory Signature of CCR2+ Monocytes and Licenses Autoimmunity. *Immunity* **43**, 502-514 (2015).

24. Cates, E.C., Fattouh, R., Wattie, J., Inman, M.D., Goncharova, S., Coyle, A.J., Gutierrez-Ramos, J.C., Jordana, M., Intranasal exposure of mice to house dust mite elicits allergic airway inflammation via a GM-CSF-mediated mechanism. *J. Immunol.* **173**, 6384-6392 (2004).

25. Yamashita, N., Tashimo, H., Ishida, H., Kaneko, F., Nakano, J., Kato, H., Hirai, K., Horiuchi, T., Ohta, K., Attenuation of airway hyperresponsiveness in a murine asthma model by neutralization of granulocyte-macrophage colony-stimulating factor (GM-CSF). *Cell. Immunol.* **219**, 92-97 (2002).

26. A. Sheih, W. C. Parks, S. F. Ziegler, GM-CSF produced by the airway epithelium is required for sensitization to cockroach allergen. *Mucosal Immunol.* **10**, 705-715 (2017).

27. Shim, D.S., Schilter, H.C., Knott, M.L., Almeida, R.A., Short, R.P., Mackay, C.R., Dent, L.A., Sewell, W.A., Protection against Nippostrongylus brasiliensis infection in mice is independent of GM-CSF. *Immunol. Cell. Biol.* **90**, 553-558 (2012).

28. Seimiya, M., Wada, A., Kawamura, K., Sakamoto, A., Ohkubo, Y., Okada, S., Hatano, M., Tokuhisa, T., Watanabe, T., Saisho, H., et al., Impaired lymphocyte development and function in Clast5/Stra13/DEC1-transgenic mice. *Eur. J. Immunol.* **34**, 1322-1332 (2004).

29. Kanda, M., Yamanaka, H., Kojo, S., Usui, Y., Honda, H., Sotomaru, Y., Harada, M., Taniguchi, M., Suzuki, N., Atsumi, T., et al., Transcriptional regulator Bhlhe40 works as a cofactor of T-bet in the regulation of IFN-γ production in iNKT cells. *Proc. Natl. Acad. Sci. U. S. A.* **113**, E3394-3402 (2016).

30. Kreslavsky, T., Vilagos, B., Tagoh, H., Poliakova, D.K., Schwickert, T.A., Wohner, M., Jaritz, M., Weiss, S., Taneja, R., Rossner, M.J., Busslinger, M., Essential role for the transcription factor Bhlhe41 in regulating the development, self-renewal and BCR repertoire of B-1a cells. *Nat. Immunol.* **18**, 442-455 (2017).

31. Camponeschi, A., Todi, L., Cristofoletti, C., Lazzeri, C., Carbonari, M., Mitrevski, M., Marrapodi, R., Del Padre, M., Fiorilli, M., Casato, M., Visentini, M. DEC1/STRA13 is a key negative regulator of activation-induced proliferation of human B cells highly expressed in anergic cells. *Immunol. Lett.* **198**, 7-11 (2018).

32. Huynh, J.P., Lin, C.C., Kimmey, J.M., Jarjour, N.N., Schwarzkopf, E.A., Bradstreet, T.R., Shchukina, I., Shpynov, O., Weaver, C.T., Taneja, R., et al., Bhlhe40 is an essential

repressor of IL-10 during Mycobacterium tuberculosis infection. *J. Exp. Med.* **215**, 1823-1838 (2018).

33. Lin, C.C., Bradstreet, T.R., Schwarzkopf, E.A., Sim, J., Carrero, J.A., Chou, C., Cook, L.E., Egawa, T., Taneja, R., Murphy, T.L., et al., Bhlhe40 controls cytokine production by T cells and is essential for pathogenicity in autoimmune neuroinflammation. *Nat. Commun.* **5**, 3551 (2014).
34. Lin, C.C., Bradstreet, T.R., Schwarzkopf, E.A., Jarjour, N.N., Chou, C., Archambault, A.S., Sim, J., Zinselmeyer, B.H., Carrero, J.A., Wu, G.F., et al., IL-1-induced Bhlhe40 identifies pathogenic T helper cells in a model of autoimmune neuroinflammation. *J. Exp. Med.* **213**, 251-271 (2016).
35. Martínez-Llordella, M., Esensten, J.H., Bailey-Bucktrout, S.L., Lipsky, R.H., Marini, A., Chen, J., Mughal, M., Mattson, M.P., Taub, D.D., Bluestone, J.A., CD28-inducible transcription factor DEC1 is required for efficient autoreactive CD4+ T cell response. *J. Exp. Med.* **210**, 1603-1619 (2013).
36. Yu, F., Sharma, S., Jankovic, D., Gurram, R.K., Su, P., Hu, G., Li, R., Rieder, S., Zhao, K., Sun, B., and Zhu, J., The transcription factor Bhlhe40 is a switch of inflammatory versus antiinflammatory Th1 cell fate determination. *J. Exp. Med.* **215**, 1813-1821 (2018).
37. Jarjour, N.N., Schwarzkopf, E.A., Bradstreet, T.R., Shchukina, I., Lin, C.C., Huang, S.C., Lai, C.W., Cook, M.E., Taneja, R., Stappenbeck, T.S., et al., Bhlhe40 mediates tissue-specific control of macrophage proliferation in homeostasis and type 2 immunity. *Nat. Immunol.* **20**, 687-700 (2019).

38. Yasuda, K., Kitagawa, Y., Kawakami, R., Isaka, Y., Watanabe, H., Kondoh, G., Kohwi-Shigematsu, T., Sakaguchi, S., Hirota, K., Satb1 regulates the effector program of encephalitogenic tissue Th17 cells in chronic inflammation. *Nat. Commun.* **10**, 549 (2019).

39. Henriksson, J., Chen, X., Gomes, T., Ullah, U., Meyer, K.B., Miragaia, R., Duddy, G., Pramanik, J., Yusa, K., Lahesmaa, R., and Teichmann, S.A., Genome-wide CRISPR Screens in T Helper Cells Reveal Pervasive Crosstalk between Activation and Differentiation. *Cell* **176**, 882-896.e18 (2019).

40. Tibbitt, C.A., Stark, J.M., Martens, L., Ma, J., Mold, J. E., Deswarte, K., Oliynyk, G., Feng, X., et al., Single-Cell RNA Sequencing of the T Helper Cell Response to House Dust Mites Defines a Distinct Gene Expression Signature in Airway Th2 Cells. *Immunity* **51**, 1-16 (2019).

41. Filbey, K.J., Grainger, J.R., Smith, K.A., Boon, L., van Rooijen, N., Harcus, Y., Jenkins, S., Hewitson, J.P., Maizels, R.M., Innate and adaptive type 2 immune cell responses in genetically controlled resistance to intestinal helminth infection. *Immunol. Cell. Biol.* **92**, 436-448 (2014).

42. Bain, C.C., Bravo-Blas, A., Scott, C.L., Perdiguero, E.G., Geissmann, F., Henri, S., Malissen, B., Osborne, L.C., Artis, D., Mowat, A.M., Constant replenishment from circulating monocytes maintains the macrophage pool in the intestine of adult mice. *Nat. Immunol.* **15**, 929-937 (2014).

43. C. L. Scott, C. C. Bain, A. M. Mowat, Isolation and Identification of Intestinal Myeloid Cells. *Methods Mol. Biol.* **1559**, 223-239 (2017).

44. Anthony, R.M., Urban, J.F., Alem, F., Hamed, H.A., Rozo, C.T., Boucher, J.L., Van Rooijen, N., Gause, W.C., Memory T(H)2 cells induce alternatively activated macrophages to mediate protection against nematode parasites. *Nat. Med.* **12**, 955-960 (2006).

45. S. Steinfelder, S. Rausch, D. Michael, A. A. Kuhl, S. Hartmann, Intestinal helminth infection induces highly functional resident memory CD4(+) T cells in mice. *Eur. J. Immunol.* **47**, 353-363 (2017).

46. K. Mohrs, D. P. Harris, F. E. Lund, M. Mohrs, Systemic dissemination and persistence of Th2 and type 2 cells in response to infection with a strictly enteric nematode parasite. *J. Immunol.* **175**, 5306-5313 (2005).

47. Chen, T., Tibbitt, C.A., Feng, X., Stark, J.M., Rohrbeck, L., Rausch, L., Sedimbi, S.K., Karlsson, M.C.I., Lambrecht, B.N., Karlsson Hedestam, G.B., et al., PPAR-gamma promotes type 2 immune responses in allergy and nematode infection. *Sci. Immunol.* **2**, (2017).

48. Chenery, A.L., Alhallaf, R., Agha, Z., Ajendra, J., Parkinson, J., Cooper, M.M., Chan, B.H.K., Eichenberger, R.M., Dent, L.A., Robertson, A.A.B., et al. *BioRxiv*, 10.1101/606392 (2019)

49. Zaiss, D.M., Yang, L., Shah, P.R., Kobie, J.J., Urban, J.F., Mosmann, T.R., Amphiregulin, a TH2 cytokine enhancing resistance to nematodes. *Science* **314**, 1746 (2006).

50. Nobs, S.P., Natali, S., Pohlmeier, L., Okreglicka, K., Schneider, C., Kurrer, M., Sallusto, F., Kopf, M., PPARgamma in dendritic cells and T cells drives pathogenic type-2 effector responses in lung inflammation. *J. Exp. Med.* **214**, 3015-3035 (2017).

51. Gabrysova, L., Alvarez-Martinez, M., Luisier, R., Cox, L.S., Sodenkamp, J., Hosking, C., Perez-Mazliah, D., Whicher, C., Kannan, Y., Potempa, K., et al., c-Maf controls immune responses by regulating disease-specific gene networks and repressing IL-2 in CD4(+) T cells. *Nat. Immunol.* **19**, 497-507 (2018).

52. Codarri, L., Gyulveszi, G., Tosevski, V., Hesske, L., Fontana, A., Magnenat, L., Suter, T., Becher, B., RORgammat drives production of the cytokine GM-CSF in helper T cells, which is essential for the effector phase of autoimmune neuroinflammation. *Nat. Immunol.* **12**, 560-567 (2011).

53. S. Esnault, E. A. Kelly, Essential Mechanisms of Differential Activation of Eosinophils by IL-3 Compared to GM-CSF and IL-5. *Crit. Rev. Immunol.* **36**, 429-444 (2016).

54. Herbst, T., Esser, J., Prati, M., Kulagin, M., Stettler, R., Zaiss, M.M., Hewitson, J.P., Merky, P., Verbeek, J.S., Bourquin, C., et al., Antibodies and IL-3 support helminth-induced basophil expansion. *Proc. Natl. Acad. Sci. U. S. A.* **109**, 14954-14959 (2012).

55. Schwartz, C., Turqueti-Neves, A., Hartmann, S., Yu, P., Nimmerjahn, F., Voehringer, D., Basophil-mediated protection against gastrointestinal helminths requires IgE-induced cytokine secretion. *Proc. Natl. Acad. Sci. U. S. A.* **111**, E5169-5177 (2014).

56. H. Sun, B. Lu, R. Q. Li, R. A. Flavell, R. Taneja, Defective T cell activation and autoimmune disorder in Stra13-deficient mice. *Nat. Immunol.* **2**, 1040-1047 (2001).

57. A. B. Bialkowska, A. M. Ghaleb, M. O. Nandan, V. W. Yang, Improved Swiss-rolling Technique for Intestinal Tissue Preparation for Immunohistochemical and Immunofluorescent Analyses. *J. Vis. Exp.* **113**, e54161 (2016).

58. Bando, J.K., Gilfillan, S., Song, C., McDonald, K.G., Huang, S.C., Newberry, R.D., Kobayashi, Y., Allan, D.S.J., Carlyle, J.R., Cella, M., Colonna, M., The Tumor Necrosis

Factor Superfamily Member RANKL Suppresses Effector Cytokine Production in Group 3 Innate Lymphoid Cells. *Immunity* **48**, 1208-1219.e1204 (2018).

59. Subramanian, A., Tamayo, P., Mootha, V.K., Mukherjee, S., Ebert, B.L., Gillette, M.A., Paulovich, A., Pomeroy, S.L., Golub, T.R., Lander, E.S., and Mesirov, J.P., Gene set enrichment analysis: a knowledge-based approach for interpreting genome-wide expression profiles. *Proc. Natl. Acad. Sci. U. S. A.* **102**, 15545-15550 (2005).

Acknowledgements: We thank N. Zhang, B. Saunders, and G. Randolph for help with microscopy and technical advice. We thank E. Lantelme, D. Brinja, and A. Mitra for help with fluorescence activated cell-sorting. We thank J. Bando for help with flow cytometry of the gut. **Funding:** This work was supported by the National Institute of Allergy and Infectious Disease (NIAID) (AI113118 and AI132653) (B.T.E.) and a Burroughs Wellcome Fund Career Award for Medical Scientists (B.T.E.). N.N.J. was supported by grant 5T32AI007163 from the NIAID. S.C.-C.H. was supported by a Case Comprehensive Cancer Center American Cancer Society IRG Award (IRG-16-186-21) and a Cleveland Digestive Diseases Research Core Center Pilot Award (P30DK097948). M.E.C. was supported by the National Science Foundation Graduate Research Fellowship program (DGE-1745038). Research reported in this publication was supported by the Washington University Institute of Clinical and Translational Sciences grant UL1TR002345 from the National Center for Advancing Translational Sciences (NCATS) of the National Institutes of Health (NIH). The content is solely the responsibility of the authors and does not necessarily represent the official view of the NIH. **Author contributions:** N.N.J designed, performed, and analyzed experiments and wrote the manuscript. E.A.S., T.R.B., M.E.C., C.-W. L., and S.J.V.D. performed experiments.

S.C.-C.H. provided reagents, protocols, and technical expertise. R.T. provided mice. T.S.S., S.J.V.D. and J.F.U. provided reagents and technical expertise. B.T.E. designed and analyzed experiments, supervised the studies, and wrote the manuscript. **Competing interests:** The authors declare no competing interests. **Data and Materials Availability:** Microarray data will be deposited in the Gene Expression Omnibus upon traditional publication.

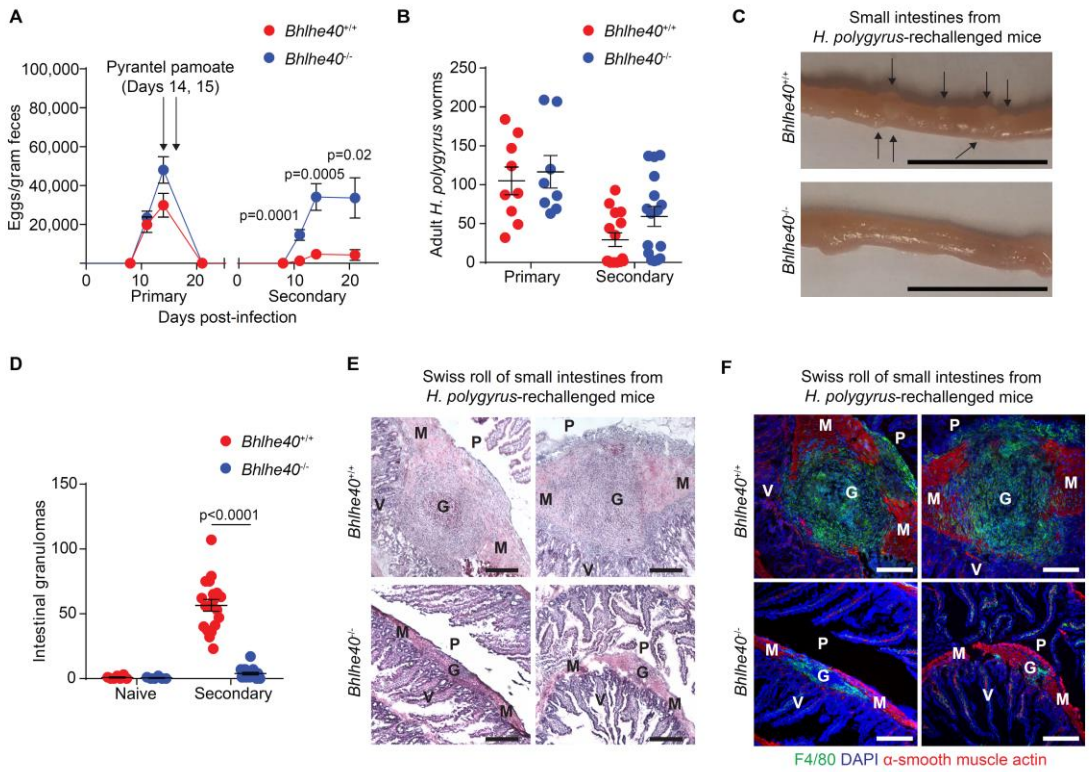

Figure 1. Bhlhe40 is required for a protective recall response to *H. polygyrus*. (A-C) *H. polygyrus*-infected *Bhlhe40*$^{+/+}$ and *Bhlhe40*$^{-/-}$ mice were analyzed for **(A)** quantitation of *H. polygyrus* eggs/gram feces over time during secondary infection, **(B)** quantitation of adult worms recovered from the intestines of mice experiencing primary or secondary infection, and **(C)** small intestine morphology after secondary infection. Arrows point to granulomas. Scale bar, 1 cm. **(D)** Quantitation of intestinal granulomas. **(E and F)** *H. polygyrus*-rechallenged *Bhlhe40*$^{+/+}$ and *Bhlhe40*$^{-/-}$ mice were analyzed histologically on adjacent sections by **(E)** hematoxylin and eosin staining and **(F)** immunostaining for F4/80, α-SMA, and DAPI performed on swiss rolls of the proximal small intestine (2 representative lesions from each genotype). G, granuloma. M, muscle layers. P, peritoneal space. V, villi. Scale bar, 200 μm. Data are representative of at least 3 independent experiments **(C, E, F)** or are pooled from at

least 3 independent experiments **(A, B, D)**. Data are mean ± s.e.m. Significance calculated with an unpaired Student's *t*-test.

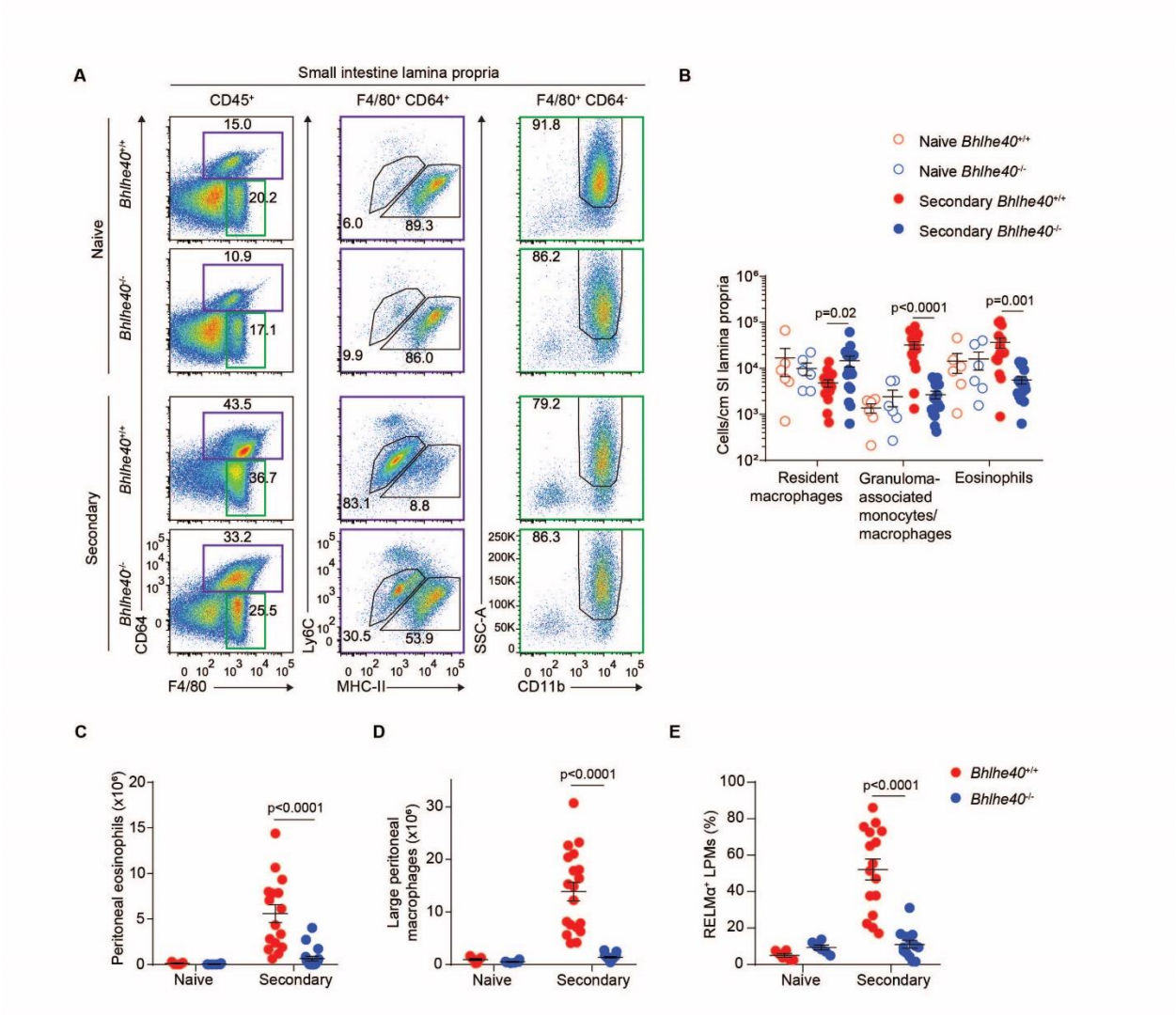

Figure 2. Bhlhe40 is required for normal myeloid cell responses to *H. polygyrus* rechallenge. (A and B) Naïve and *H. polygyrus*-rechallenged *Bhlhe40*$^{+/+}$ and *Bhlhe40*$^{-/-}$ mice were analyzed by flow cytometry for **(A)** SILP myeloid cells and **(B)** quantitation as in **(A)**. **(C-E)** Naïve and *H. polygyrus*-rechallenged *Bhlhe40*$^{+/+}$ and *Bhlhe40*$^{-/-}$ mice were analyzed by flow cytometry for quantitation of **(C)** peritoneal eosinophils, **(D)** LPMs, and **(E)** the frequency of RELMα^{+} LPMs. Data are representative of at least 3 independent experiments **(A)** or are pooled from at least 3 independent experiments **(B-E)**. Data are mean ± s.e.m. Significance calculated with an unpaired Student's *t*-test.

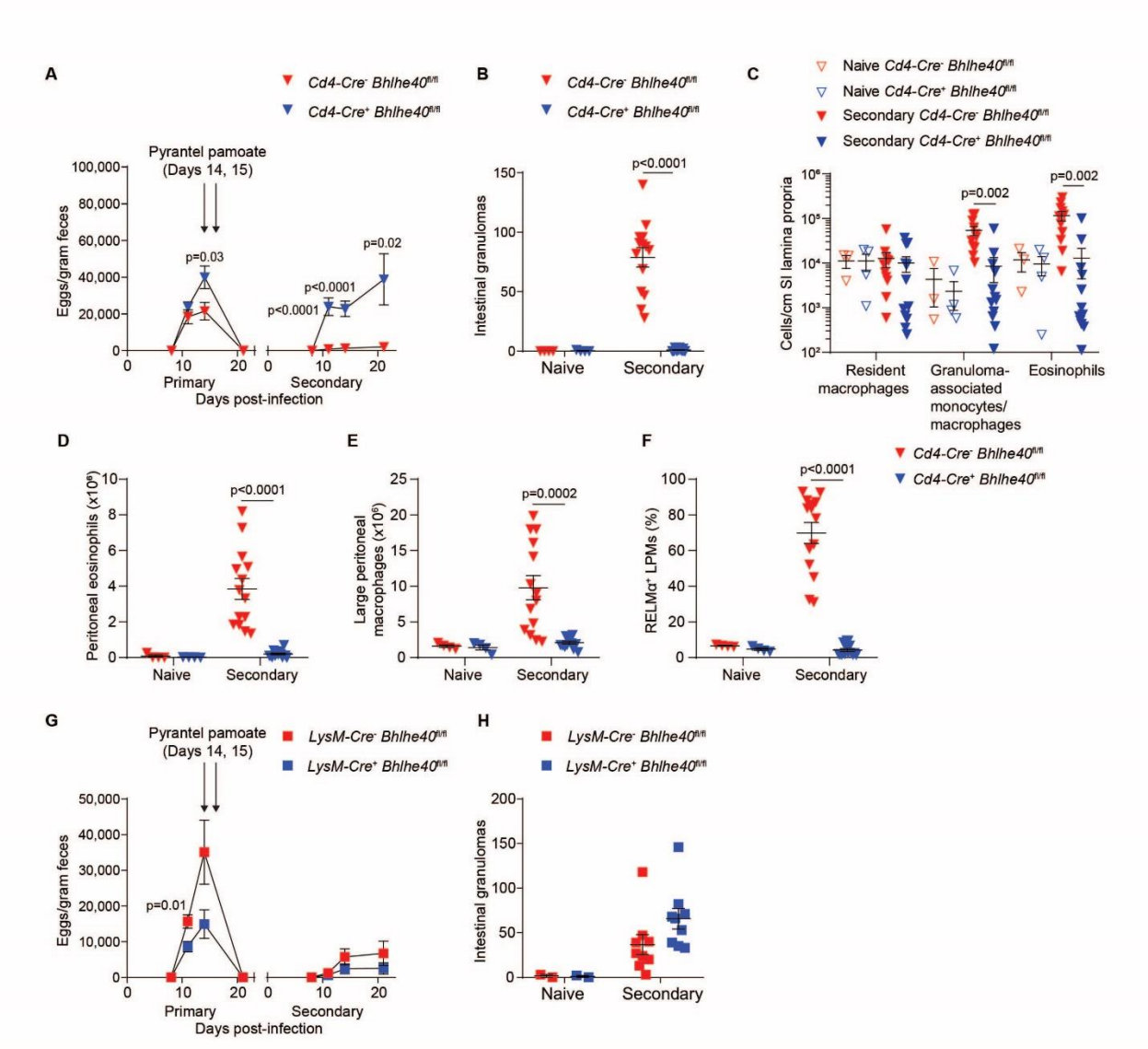

Figure 3. Bhlhe40 is required in T cells for a normal memory response to *H. polygyrus*. (A) *H. polygyrus*-rechallenged *Cd4-Cre*$^{-}$ *Bhlhe40*$^{fl/fl}$ and *Cd4-Cre*$^{+}$ *Bhlhe40*$^{fl/fl}$ mice were analyzed for quantitation of *H. polygyrus* eggs/gram feces over time. **(B)** Naïve and *H. polygyrus*-rechallenged *Cd4-Cre*$^{-}$ *Bhlhe40*$^{fl/fl}$ and *Cd4-Cre*$^{+}$ *Bhlhe40*$^{fl/fl}$ mice were analyzed for quantitation of intestinal granulomas. **(C-F)** Naïve and *H. polygyrus*-rechallenged *Cd4-Cre*$^{-}$ *Bhlhe40*$^{fl/fl}$ and *Cd4-Cre*$^{+}$ *Bhlhe40*$^{fl/fl}$ mice were analyzed by flow cytometry for quantitation of **(C)** SILP myeloid cells, **(D)** peritoneal eosinophils, **(E)** LPMs, and **(F)** the frequency of

RELMα^{+} LPMs. **(G)** *H. polygyrus*-rechallenged *LysM-Cre*$^{-}$ *Bhlhe40*$^{fl/fl}$ and *LysM-Cre*$^{+}$ *Bhlhe40*$^{fl/fl}$ mice were analyzed for quantitation of *H. polygyrus* eggs/gram feces over time. **(H)** Naïve and *H. polygyrus*-rechallenged *LysM-Cre*$^{-}$ *Bhlhe40*$^{fl/fl}$ and *LysM-Cre*$^{+}$ *Bhlhe40*$^{fl/fl}$ mice were analyzed for quantitation of intestinal granulomas. Data are pooled from 3 independent experiments **(A-F)** or 2 independent experiments **(G and H)**. Data are mean ± s.e.m. Significance calculated with an unpaired Student's *t*-test.

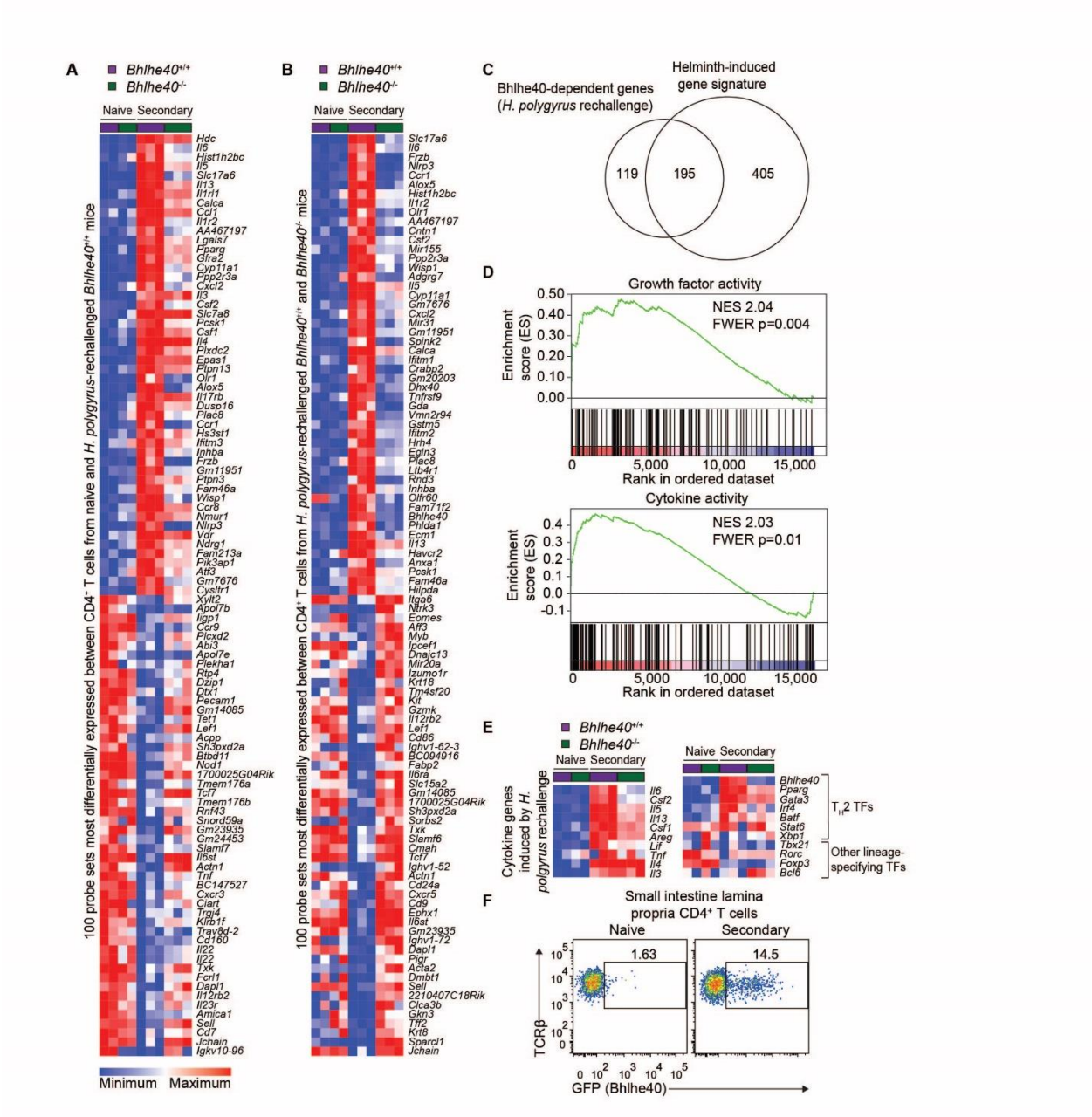

Figure 4. Loss of Bhlhe40 dysregulates the CD4⁺ T cell transcriptional response to *H. polygyrus* rechallenge. (A and B) Gene expression microarray data were analyzed for the 100 most differentially expressed probe sets in SILP CD4⁺ T cells from **(A)** naïve and *H. polygyrus*-rechallenged *Bhlhe40*$^{+/+}$ mice and **(B)** *H. polygyrus*-rechallenged *Bhlhe40*$^{+/+}$ and *Bhlhe40*$^{-/-}$ mice. **(C)** Gene expression microarray data were analyzed for shared and unique Bhlhe40-

dependent genes (≥2-fold differentially expressed between SILP CD4$^+$ T cells from *H. polygyrus*-rechallenged *Bhlhe40*$^{+/+}$ and *Bhlhe40*$^{-/-}$ mice) with the helminth-induced signature (≥2-fold differentially expressed between SILP CD4$^+$ T cells from naïve and *H. polygyrus*-rechallenged *Bhlhe40*$^{+/+}$ mice), depicted as a Venn diagram. **(D)** GSEA of gene expression microarray data for selected C5 gene sets enriched in *Bhlhe40*$^{+/+}$ versus *Bhlhe40*$^{-/-}$ SILP CD4$^+$ T cells from *H. polygyrus*-rechallenged mice. NES, normalized enrichment score. FWER, family-wise error rate. **(E)** Gene expression microarray data were analyzed for (left) expression of cytokines induced by *H. polygyrus* rechallenge and (right) expression of T_H2 and T helper cell lineage-specifying transcription factors in SILP CD4$^+$ T cells from naïve and *H. polygyrus*-rechallenged *Bhlhe40*$^{+/+}$ and *Bhlhe40*$^{-/-}$ mice. TF, transcription factor. **(F)** Flow cytometry of *Bhlhe40*^{GFP} transgene reporter expression in SILP CD4$^+$ T cells from *Bhlhe40*$^{GFP+}$ mice. Data in **(F)** are representative of 2 independent experiments. Microarray data are from a single experiment.

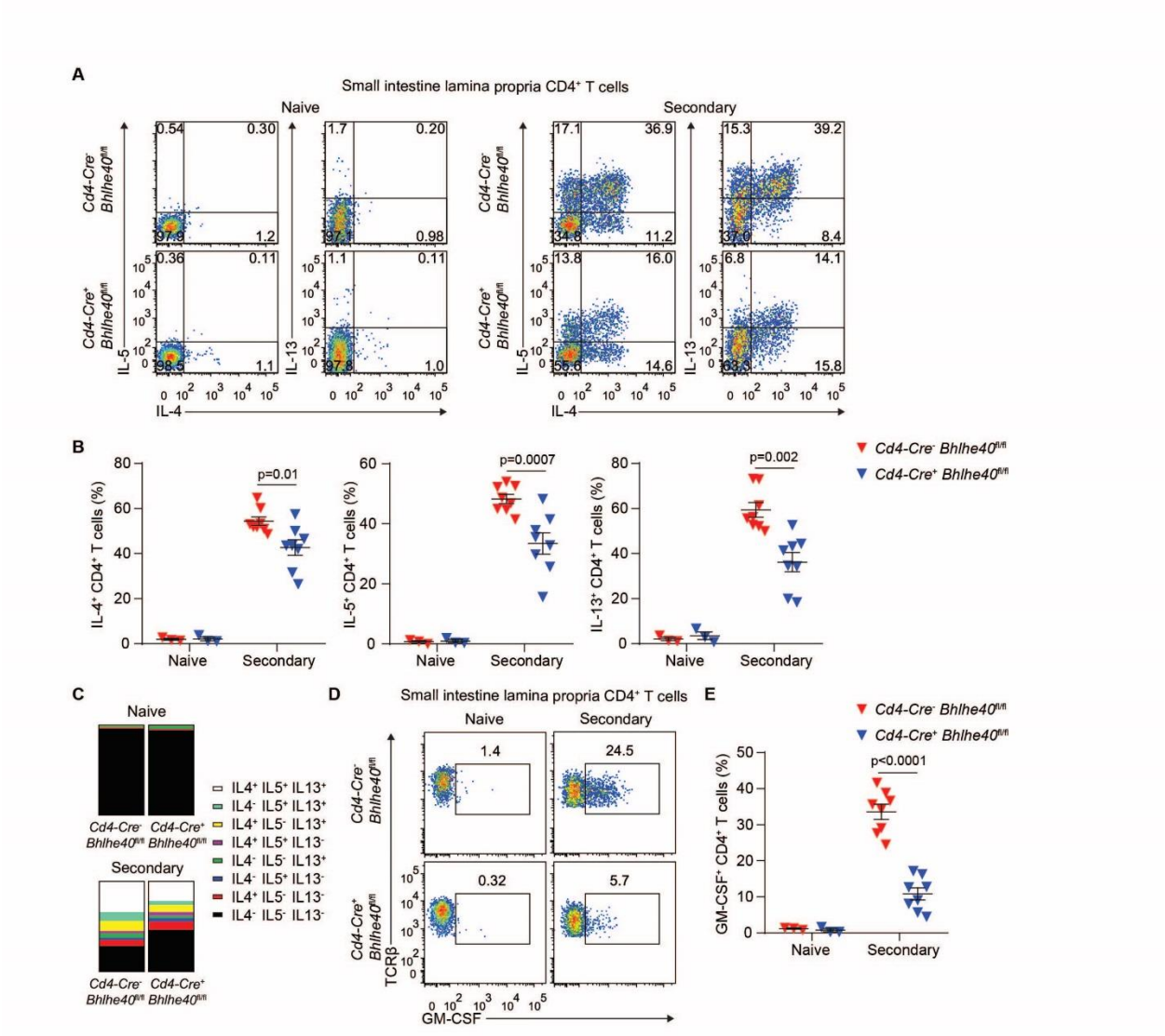

Figure 5. Bhlhe40 is required for normal CD4$^+$ T cell production of β_C chain-dependent cytokines. (A-C) Naïve and *H. polygyrus*-rechallenged *Cd4-Cre$^-$ Bhlhe40$^{fl/fl}$* and *Cd4-Cre$^+$ Bhlhe40$^{fl/fl}$* mice were analyzed by flow cytometry for **(A)** IL-4-, IL-5-, and IL-13-producing CD4$^+$ T cells, **(B)** quantitation of the frequency of IL-4$^+$, IL-5$^+$, and IL-13$^+$ CD4$^+$ T cells, and **(C)** quantitation of the frequency of CD4$^+$ T cells producing one or more cytokines after *in vitro* PMA/ionomycin stimulation of SILP cells. **(D and E)** Naïve and *H. polygyrus*-rechallenged *Cd4-Cre$^-$ Bhlhe40$^{fl/fl}$* and *Cd4-Cre$^+$ Bhlhe40$^{fl/fl}$* mice were analyzed by flow

cytometry for **(D)** GM-CSF-producing $CD4^+$ T cells and **(E)** quantitation as in **(D)** after *in vitro* PMA/ionomycin stimulation of SILP cells. Data are representative of 2 independent experiments **(A and D)** or are pooled from 2 independent experiments **(B, C, E)**. Data are mean ± s.e.m. Significance calculated with an unpaired Student's *t*-test.

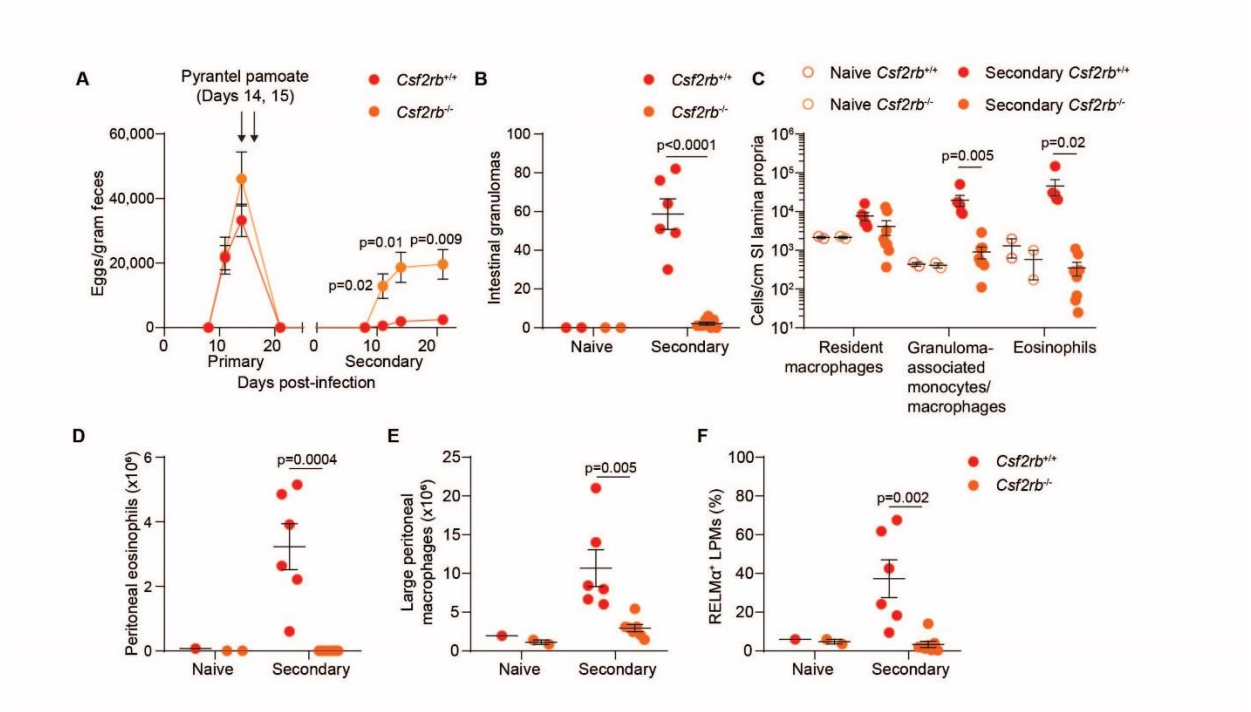

Figure 6. The βc chain is necessary for control of *H. polygyrus* rechallenge. (A) *H. polygyrus*-rechallenged *Csf2rb*$^{+/+}$ and *Csf2rb*$^{-/-}$ mice were analyzed for quantitation of *H. polygyrus* eggs/gram feces over time. **(B)** Naïve and *H. polygyrus*-rechallenged *Csf2rb*$^{+/+}$ and *Csf2rb*$^{-/-}$ mice were analyzed for quantitation of intestinal granulomas. **(C-F)** Naïve and *H. polygyrus*-rechallenged *Csf2rb*$^{+/+}$ and *Csf2rb*$^{-/-}$ mice were analyzed by flow cytometry for quantitation of **(C)** SILP myeloid cells, **(D)** peritoneal eosinophils, **(E)** LPMs, and **(F)** the frequency of RELMα^{+} LPMs. Data are pooled from 2 independent experiments. Data are mean ± s.e.m. Significance calculated with an unpaired Student's *t*-test.

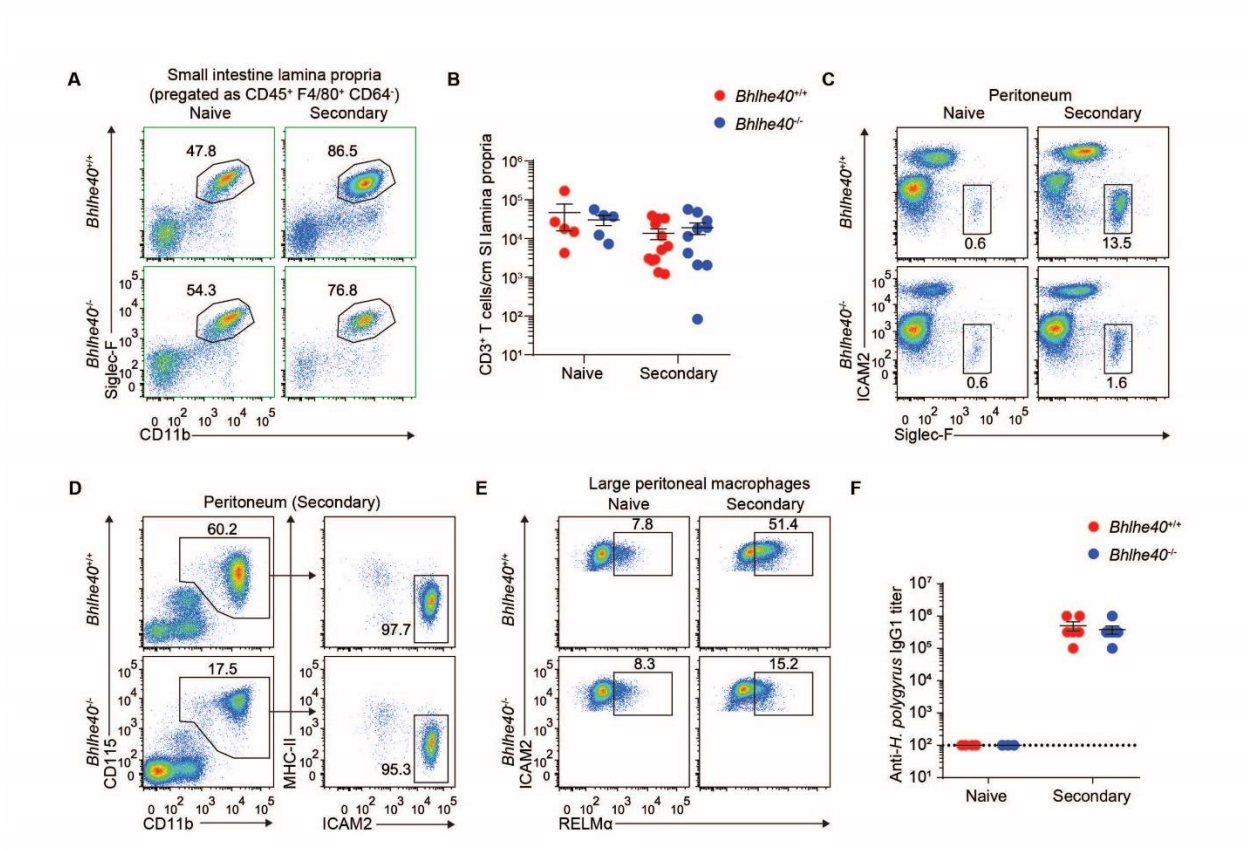

Figure S1. Loss of Bhlhe40 dysregulates myeloid cell responses to *H. polygyrus* rechallenge. (A and B) Naïve and *H. polygyrus*-rechallenged *Bhlhe40*$^{+/+}$ and *Bhlhe40*$^{-/-}$ mice were analyzed by flow cytometry for **(A)** SILP eosinophils and **(B)** quantitation of SILP CD3^{+} T cells. **(C-E)** Naïve and *H. polygyrus*-rechallenged *Bhlhe40*$^{+/+}$ and *Bhlhe40*$^{-/-}$ mice were analyzed by flow cytometry for **(C)** peritoneal eosinophils, **(D)** LPMs, and **(E)** RELMα-expressing LPMs. **(F)** Naïve and *H. polygyrus*-rechallenged *Bhlhe40*$^{+/+}$ and *Bhlhe40*$^{-/-}$ mice were analyzed for serum anti-*H. polygyrus* IgG1 titers. Data are representative of at least three independent experiments **(A, C-E)** or are pooled from at least 3 independent experiments **(B)** or 2 independent experiments **(F)**. Data are mean ± s.e.m. Significance calculated with an unpaired Student's *t*-test.

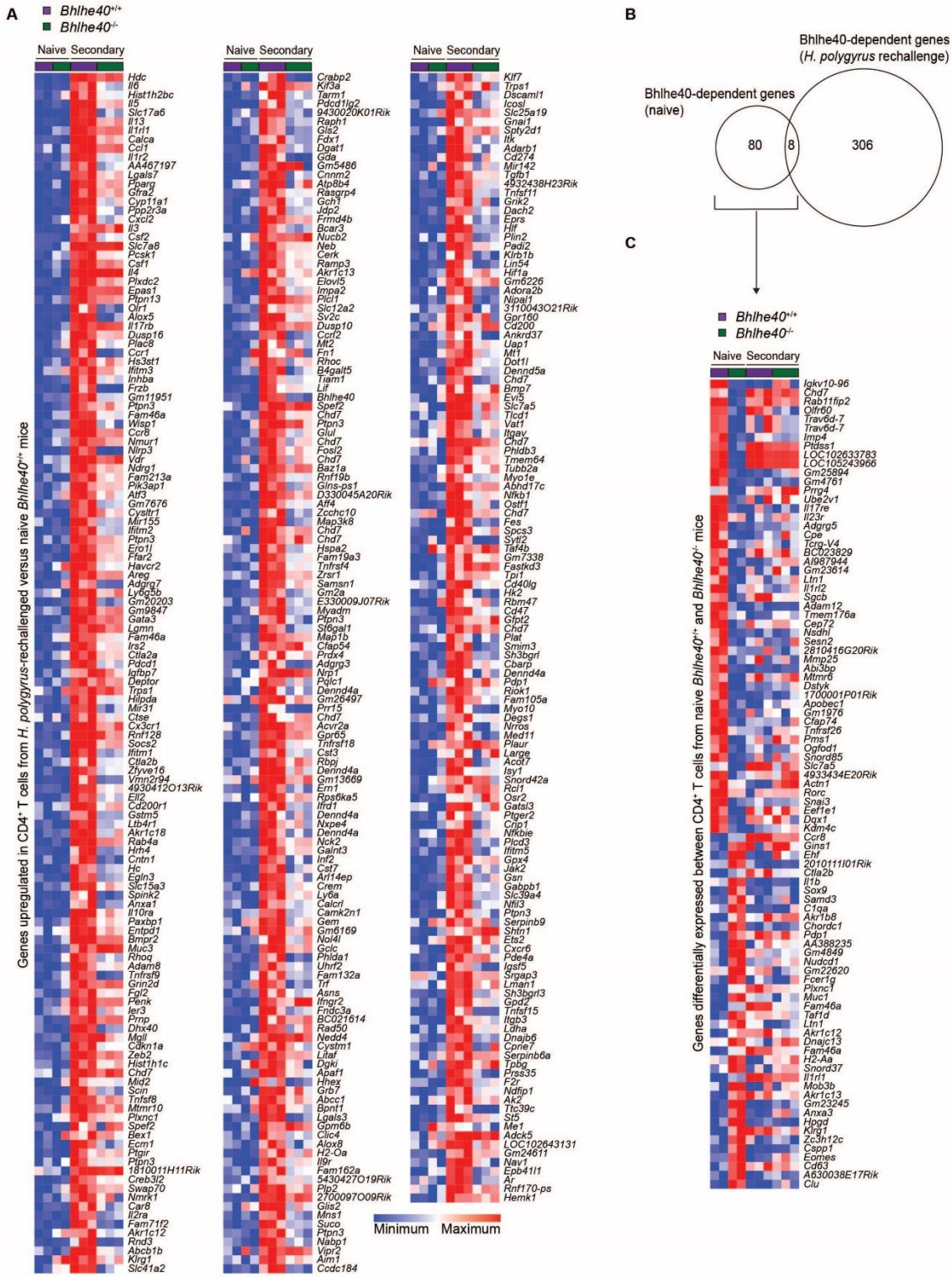
A
Bhlhe40+/+
Bhlhe40-/-
Naive Secondary
Genes upregulated in CD4+ T cells from H. polygyrus-rechallenged versus naive Bhlhe40+/+ mice
Minimum Maximum
B
Bhlhe40-dependent genes (H. polygyrus rechallenge)
Bhlhe40-dependent genes (naive)
80
8
306
C
Genes differentially expressed between CD4+ T cells from naive Bhlhe40+/+ and Bhlhe40-/- mice

Figure S2. Bhlhe40 regulates distinct gene sets in CD4$^+$ T cells from naïve and *H. polygyrus*-rechallenged mice. (A) Gene expression microarray data were analyzed for genes induced by ≥2-fold in SILP CD4$^+$ T cells from *H. polygyrus*-rechallenged as compared to naïve *Bhlhe40*$^{+/+}$ mice. **(B)** Gene expression microarray data were analyzed for shared and unique Bhlhe40-dependent genes (≥2-fold differentially expressed) in SILP CD4$^+$ T cells from naïve or *H. polygyrus*-rechallenged *Bhlhe40*$^{+/+}$ and *Bhlhe40*$^{-/-}$ mice, depicted as a Venn diagram. **(C)** Gene expression microarray data were analyzed for genes differentially expressed by ≥2-fold in SILP CD4$^+$ T cells from naïve *Bhlhe40*$^{+/+}$ and *Bhlhe40*$^{-/-}$ mice. Microarray data are from a single experiment.

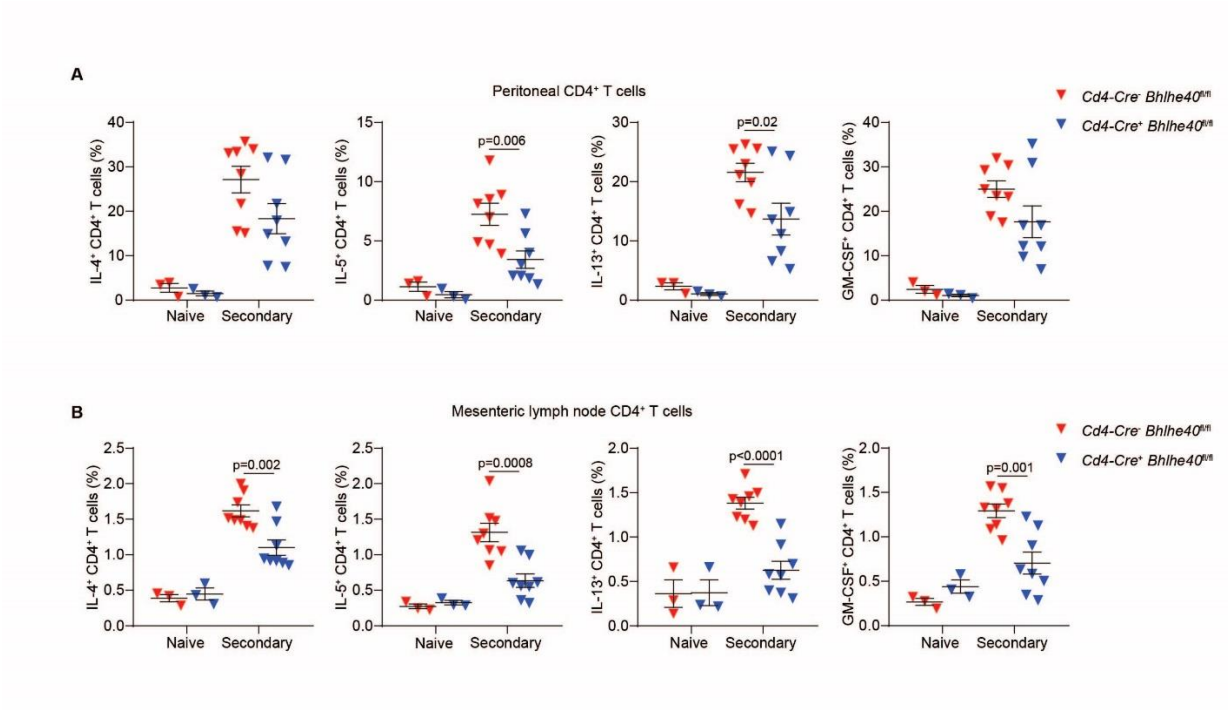

Figure S3. Bhlhe40 is required in T cells for normal cytokine production during *H. polygyrus* rechallenge. (A and B) Naïve and *H. polygyrus*-rechallenged *Cd4-Cre*$^{-}$ *Bhlhe40*$^{fl/fl}$ and *Cd4-Cre*$^{+}$ *Bhlhe40*$^{fl/fl}$ mice were analyzed by flow cytometry for quantitation of the frequency of IL-4^{+}, IL-5^{+}, IL-13^{+}, and GM-CSF^{+} CD4^{+} T cells from the **(A)** peritoneal cavity and **(B)** mesenteric lymph nodes after *in vitro* PMA/ionomycin stimulation. Data are pooled from 2 independent experiments. Data are mean ± s.e.m. Significance calculated with an unpaired Student's *t*-test.

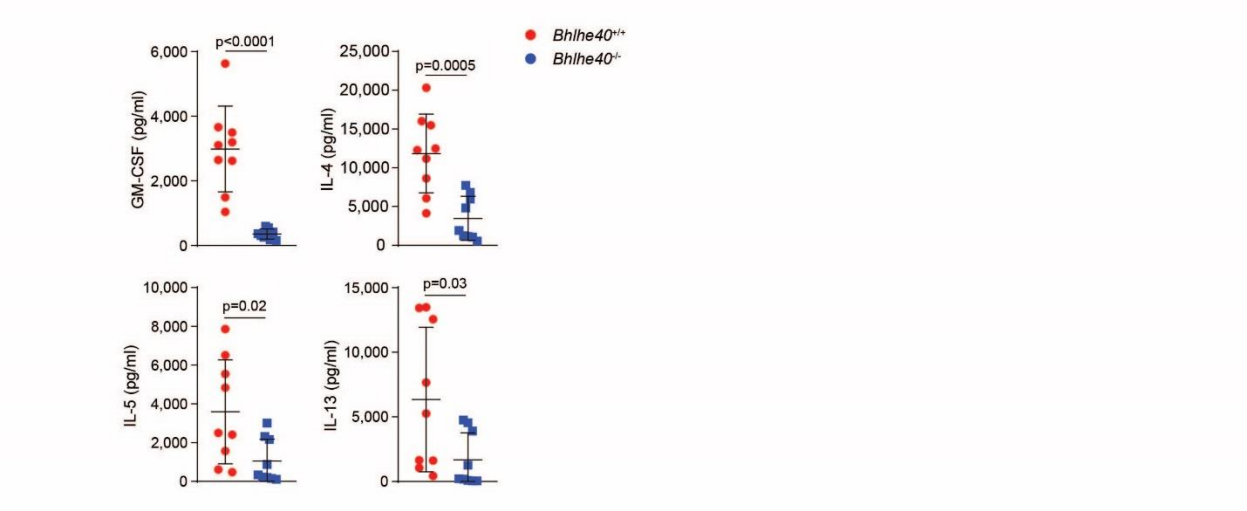

Figure S4. *In vitro*-polarized T_H2 cells require Bhlhe40 for normal cytokine production. Naïve $CD4^+$ T cells from *Bhlhe40*$^{+/+}$ and *Bhlhe40*$^{-/-}$ mice were differentiated in culture into T_H2 cells and restimulated to assess production of GM-CSF, IL-4, IL-5, and IL-13 by ELISA. Data are pooled from 3 independent experiments. Data are mean ± s.e.m. Significance calculated with an unpaired Student's *t*-test.

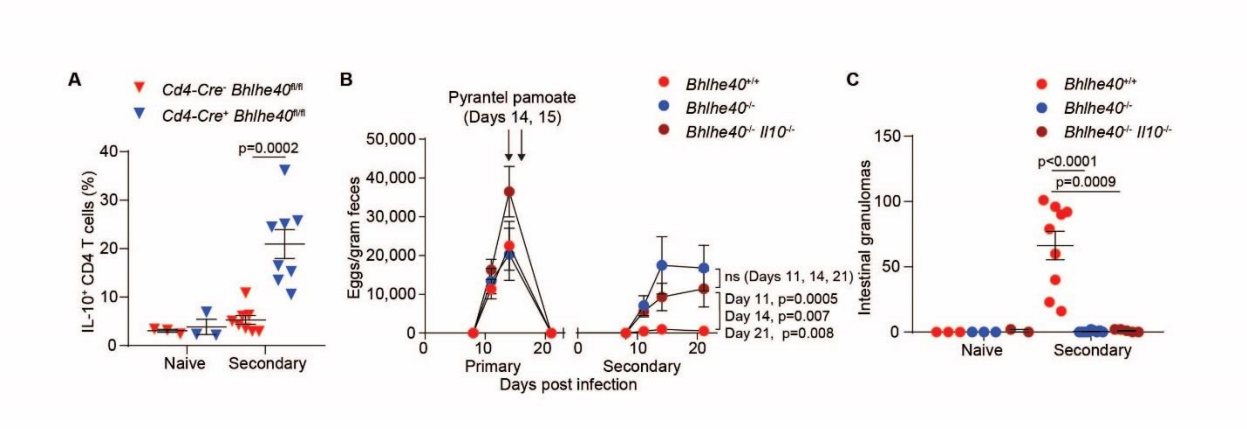

Figure S5. Genetic deletion of IL-10 in *Bhlhe40*$^{-/-}$ *Il10*$^{-/-}$ mice does not restore control of *H. polygyrus* rechallenge. (A) Naïve and *H. polygyrus*-rechallenged *Cd4-Cre*$^{-}$ *Bhlhe40*$^{fl/fl}$ and *Cd4-Cre*$^{+}$ *Bhlhe40*$^{fl/fl}$ mice were analyzed by flow cytometry for quantitation of the frequency of IL-10^{+} CD4^{+} T cells after *in vitro* PMA/ionomycin stimulation of SILP cells. **(B)** *H. polygyrus*-rechallenged *Bhlhe40*$^{+/+}$, *Bhlhe40*$^{-/-}$, and *Bhlhe40*$^{-/-}$ *Il10*$^{-/-}$ mice were analyzed for quantitation of *H. polygyrus* eggs/gram feces over time. **(C)** Naïve and *H. polygyrus*-rechallenged *Bhlhe40*$^{+/+}$, *Bhlhe40*$^{-/-}$, and *Bhlhe40*$^{-/-}$ *Il10*$^{-/-}$ mice were analyzed for quantitation of intestinal granulomas. Data are pooled from 2 independent experiments. Data are mean ± s.e.m. Significance calculated with an unpaired Student's *t*-test.

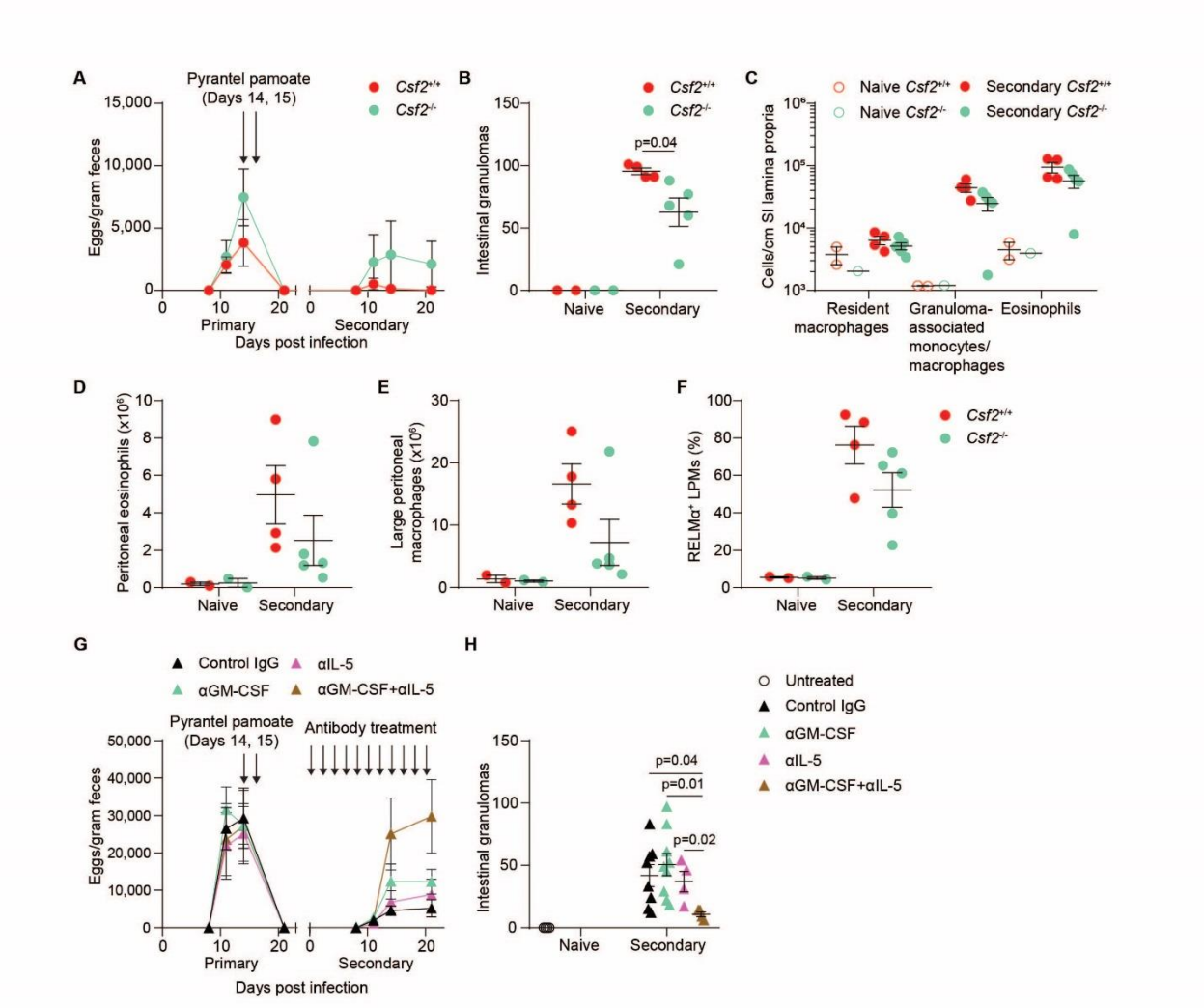

Figure S6. Combined deficiency in IL-5 and GM-CSF results in impaired control of *H. polygyrus* rechallenge. (A) *H. polygyrus*-rechallenged *Csf2*$^{+/+}$ and *Csf2*$^{-/-}$ mice were analyzed for quantitation of *H. polygyrus* eggs/gram feces over time. **(B)** Naïve and *H. polygyrus*-rechallenged *Csf2*$^{+/+}$ and *Csf2*$^{-/-}$ mice were analyzed for quantitation of intestinal granulomas. **(C)** Naïve and *H. polygyrus*-rechallenged *Csf2*$^{+/+}$ and *Csf2*$^{-/-}$ mice were analyzed by flow cytometry for quantitation of SILP myeloid cells. **(D-F)** Naïve and *H. polygyrus*-rechallenged *Csf2*$^{+/+}$ and *Csf2*$^{-/-}$ mice were analyzed by flow cytometry for quantitation of **(D)** peritoneal eosinophils, **(E)** LPMs, and **(F)** the frequency of RELMα^{+} LPMs. **(G)** Wild type mice were

rechallenged with *H. polygyrus* concurrent with control IgG, αGM-CSF, αIL-5, or αGM-CSF plus αIL-5 antibody treatment and were analyzed for quantitation of *H. polygyrus* eggs/gram feces over time. **(H)** Naïve (open circles) and *H. polygyrus*-rechallenged mice (filled triangles) treated as in **(G)** were analyzed for quantitation of intestinal granulomas. Data are from single experiments. Data are mean ± s.e.m. Significance calculated with an unpaired Student's *t*-test.

Table S1

Antibodies and fluorescent dyes

Antigen and fluorophore	Vendor	Clone	Catalog	Application
α-SMA Cy3	Sigma	1A4	Cat# C6198	Immunofluorescence
CD3ε APC/Cy7	BioLegend	17A2	Cat# 100222	Flow cytometry
CD4 PE/Cy7	BioLegend	RM4-5	Cat# 100528	Flow cytometry
CD4 BV510	BioLegend	RM4-5	Cat# 100559	Flow cytometry
CD8a PerCP/Cy5.5	Tonbo	53-6.7	Cat# 65-0081	Flow cytometry
CD8a APC/Cy7	Tonbo	53-6.7	Cat# 25-0081	Flow cytometry
CD11b PE/Cy7	BioLegend, Tonbo	M1/70	Cat# 101216, 60-0112	Flow cytometry
CD11b APC/Cy7	BioLegend, Tonbo	M1/70	Cat# 101226, 25-0112	Flow cytometry
CD16/32	BioXCell	2.4G2	Cat# BE0008	Flow cytometry (Fcblock)
CD19 PerCP/Cy5.5	Tonbo	1D3	Cat# 65-0193	Flow cytometry
CD45 BV510	BD	30-F11	Cat# 563891	Flow cytometry
CD45 RF710	Tonbo	30-F11	Cat# 80-0451	Flow cytometry
CD45.2 FITC	BioLegend	104	Cat# 109806	Flow cytometry
CD64 APC	BioLegend	X54-5/7.1	Cat# 139306	Flow cytometry
CD102 FITC	BioLegend	3C4 (MIC2/4)	Cat# 105606	Flow cytometry
CD102 AF647	BioLegend	3C4 (MIC2/4)	Cat# 105612	Flow cytometry
CD115 PE	Tonbo	AFS98	Cat# 50-1152	Flow cytometry
CD115 BV421	BioLegend	AFS98	Cat# 135513	Flow cytometry
F4/80 AF647	BioLegend	BM8	Cat# 123121	Immunofluorescence
F4/80 PerCP/Cy5.5	Tonbo	BM8.1	Cat# 65-4801	Flow cytometry
GM-CSF	Leinco	MP1-22E9	Cat# G670	In vivo neutralization
GM-CSF BV421	BD	MP1-22E9	Cat# 564747	Flow cytometry
Goat α-Rabbit AF647	Life Technologies	polyclonal (A21245)	Cat# A21245	Flow cytometry
I-A/I-E BV510	BioLegend	M5/114.15.2	Cat# 107635	Flow cytometry
I-A/I-E PB	BioLegend	M5/114.15.2	Cat# 107620	Flow cytometry
I-A/I-E RF710	Tonbo	M5/114.15.2	Cat# 80-5321	Flow cytometry
IL-4 APC	BioLegend	11B11	Cat# 504105	Flow cytometry
IL-5	BioXCell	TRFK5	Cat# BE0198	In vivo neutralization
IL-5 BV421	BioLegend	TRFK5	Cat# 504311	Flow cytometry
IL-10 APC	BioLegend	JES5-16E3	Cat# 505010	Flow cytometry
IL-13 PE/Cy7	eBioscience	eBio13A	Cat# 25-7133	Flow cytometry
Ly6C APC/Cy7	BioLegend	HK1.4	Cat# 128026	Flow cytometry
Ly6C BV510	BioLegend	HK1.4	Cat# 128033	Flow cytometry
Polyclonal rat IgG	Sigma	NA (I4131)	Cat# I4131	In vivo neutralization
RELMα	Peprotech	polyclonal (500-P214)	Cat# 500-P214	Flow cytometry
Siglec-F PE	BD	E50-2440	Cat# 552126	Flow cytometry
TCRβ (H57-597) PE	BioLegend	H57-597	Cat# 109208	Flow cytometry

Reagent	Vendor	Clone	Catalog	Application
Streptavidin	PE, PerCP/Cy5.5, PE/Cy7, APC, APC/e780, V500, V450	NA	Various	Flow cytometry
Fluoroshield mounting medium with DAPI	Abcam	NA	Cat# ab104139	Immunofluorescence
C57BL/6 Mouse Immunoglobulin Panel	SouthernBiotech	NA	Cat# 5300-01B	ELISA
Biotin anti-mouse GM-CSF	BioLegend	MP1-31G6	Cat# 505502	ELISA
Purified anti-mouse GM-CSF	BioLegend	MP1-22E9	Cat# 505402	ELISA
Murine GM-CSF	Peprotech	NA	Cat# 315-03	ELISA
Mouse IL-4 ELISA Max Standar	BioLegend	NA	Cat# 431101	ELISA
Mouse IL-5 ELISA Max Standar	BioLegend	NA	Cat# 431201	ELISA
Mouse IL-13 DuoSet ELISA	R&D	NA	DY413	ELISA